



UNIVERSITAT
POLITÈCNICA
DE VALÈNCIA



ETSI Aeroespacial y Diseño Industrial



Univerza v Mariboru



Fakulteta za
strojništvo

Analysis of different approaches for the reduction of NO_x in a hydrogen fuelled internal combustion engine.

Student: Marcos Mas Arroyo
Study programme: Bachelor's degree in mechanical engineering.
Mentor UPV: Prof. Dr. Jaime Martín Díaz
Mentor UM: Assistant. Prof. Dr. Luka Lešnik

Maribor, July 2024

Abstract

The threat posed by climate change and energy security crisis has stimulated the response of the governments, which are putting strategic plans in motion to promote alternative energy sources that protect the planet, rather than the current petroleum and carbon-based fuels. This initiative promotes research focused on sustainable transport and the reduction of greenhouse gas emission. Traditional fuels such as gasoline and diesel are being phased out in favour of alternatives fuels and new ways of mobility. Hydrogen, in particular, offers a promising solution because of its virtually zero CO₂ emissions during combustion, although it can still produce nitrogen oxides (NO_x).

The work consists in analyse different approaches to obtain really low or nearly zero NO_x emissions in a Hydrogen internal combustion engine (H₂ICE) without obtaining an efficiency far from the current ICE on the market. To analyse the performance and emission trends of an engine a simulation study with AVL BOOST will be conducted. Starting from a model of the program examples which will be adapted to hydrogen fuel, whereby the compression ratio can be variated; taking advantage of the wide flammability limits of hydrogen, different strategies on the equivalence ratio ($1/\lambda$) will be discussed, also will be consider the possibility of introducing chargers or turbochargers to allow lean mixtures and proper efficiency. Finally, the challenges for reaching these goals and the future trends are discussed.

Acknowledgment

Firstly, I would like to thank my mentor for giving me the opportunity to undertake this kind of work and for always being willing to help.

I would also like to thank my family and friends for everything they have taught me and made me who I am today; for always putting up with me and supporting me, no matter what time it is.

(Me gustaría agradecer también a mi familia y amigos por todo lo que me han enseñado y me ha hecho ser quien soy; por aguantarme y apoyarme siempre, sea la hora que sea.)

Papá, Mamá, Jose mil gracias por todo lo que me ha habéis dado directa o indirectamente, me dais fuerza y me hacéis ser mejor a todos los niveles. En nada estamos de vuelta.

In general, thank you all for accompanying me in this beautiful story in which we finish a stage and start a new one with excitement and hunger.

Index

Index of Figures.....	4
Index of Tables.....	6
1. Introduction.....	7
1.1. Background.....	7
1.2. Assumptions and constraints.....	9
1.3. Scope of the work.....	9
2. Hydrogen.....	10
2.1. Properties of the hydrogen	10
2.2. Production processes and classification of hydrogen according to these processes	14
2.3. Ways of storage the hydrogen and its safety.....	18
3. Abnormal combustion problems to avoid in a H2ICE.....	19
4. Justification of engine base line used.....	21
5. Justification of induction technique used.....	21
6. Methodology	24
6.1. Introduction to the program AVL BOOST™ and its parts.....	24
6.2. Justification of elected type of ICE.....	25
6.3. Choice of the combustion model used in the simulation.....	26
6.3.1. Vibe function / Wiebe function.....	26
6.4. Analysis of in-cylinder pressure.....	28
6.4.1. ROHR of Hydrogen from literature	30
6.5. Curve fitting.....	30
6.6. Simulation parameters and approaches.....	36
6.7. Simulation results of the hydrogen engine	37
6.7.1. Reference values with the Gasoline Model.....	37
6.7.2. NO _x Emissions Reduction Strategies.....	38
6.7.3. Influence of emission reduction strategies on performance.....	41
6.7.4. Turbocharger implementation	43
6.7.5. Testing of reduction strategies with turbocharger	46
6.7.6. Combination of strategies	48
7. Conclusions	51
REFERENCIAS	53
ANNEX A: Boundary condition and initialization set up.....	55
ANNEX B: Vibe parameters fitted.....	68
ANNEX C: Simulation results gathered to evaluate the different approaches.....	0

Index of Figures

Figure 1: Minimum ignition energy for hydrogen and methane [7].	12
Figure 2: Classification of Hydrogen in colours from the Sustainable NI blog [21].	16
Figure 3: Simplified classification of hydrogen colours from the United Nations Economic Commission for Europe Committee on Sustainable Energy (UNECE) [22].	16
Figure 4: The Hydrogen colour wheel by Mitsubishi Heavy Industries Group [4].	17
Figure 5: Demonstration of hydrogen safety: hydrogen fire (left) versus gasoline fire (right) [7]	19
Figure 6: Comparison of specific power density of hydrogen mixture formation [25].	22
Figure 7: Explanation of the main window with a model from examples.	24
Figure 8: Basic model used for the simulations. It is based on figure 7 model.	25
Figure 9: Vibe 2-zone section in the menu of combustion inside the cylinder element.	27
Figure 10: Results of in-cylinder pressure for different lambdas. The marks are the experimental values from S. Verhelst and Sierens [26].	28
Figure 11: Target Pressure Curve two-zone combustion model menu inside cylinder element.	29
Figure 12: Comparison of Reat of Heat Release between Excel estimation in red and pressure analysis results.	29
Figure 13: In-cylinder pressure and ROHR at different lambdas for engine speeds of 2000 rpm (left) and 3000 rpm (right) [17].	30
Figure 14: Fragment of the fitting script. Initialization	31
Figure 15: Fragment of the fitting script. Where the loop is implemented for 1000 iteration to find a proper minimum.	33
Figure 16: Example of the error in the extrapolation.	35
Figure 17: Gasoline performance.	37
Figure 18: Gasoline efficiency.	37
Figure 19: Gasoline NO _x Emissions	38
Figure 20: Influence of Lean-burn approach on engine performance.	39
Figure 21: Influence of Lean-burn approach on efficiency for 2000 rpm (a) and 3000 rpm (b) at CR=11.5 cases.	39
Figure 22: Influence of Lean-burn on NO _x Emissions at 2000 rpm and CR 11.5.	39
Figure 23: Influence of Lean-burn on NO _x Emissions at 3000 rpm and CR 11.5.	40
Figure 24: Influence of the change of CR on NO _x Emissions at 2000 rpm and lambda = 2.	40
Figure 25: Influence of the change of CR on the efficiency at 2000 rpm and lambda = 2.	41
Figure 26: Influence of the change of CR on the performance at 2000 rpm and lambda = 2	41
Figure 27: Comparison of the influence of both approaches of reduction emission on the performance.	42
Figure 28: Modification of the model to include a Turbocharged and intercooler.	43
Figure 29: Compressor Mass Flow for different Pressure Boost (PB) at 2000rpm, Lambda = 2 and CR = 9 from simulations applying compression ratio reduction (Section 6.7.5.1)	44
Figure 30: Influence of the TCI system in the NO _x emissions.	44
Figure 31: influence of Turbocharger on the efficiency for lambda = 2 and CR = 11.5; a) efficiency at 2000 rpm; b) efficiency at 3000 rpm; c) comparation of efficiencies	45

Figure 32: Influence of the Pressure Boost in the BEMP and Torque at 2000 rpm, Lambda = 2 and CR = 11.5.....	46
Figure 33: Consideration of engine speed in the analysis of the NO _x emissions after the introduction of the TCI system, data obtain at Lambda = 2.8 and CR = 11.5.	48
Figure 34: Brake efficiency comparison at 2000 rpm between the different cases studied after the introduction of the TCI system. Blue for baseline, orange for CR reduction and green for Lean-burn approach.	48
Figure 35: Brake efficiency comparison at 2000 rpm between the reference in the TCI (blue) and the combination approaches for two different lambdas.....	49
Figure 36: Simulation Control: Cycle Simulation.....	55
Figure 37: Engine: Friction set.....	56
Figure 38: Air Cleaner: General	56
Figure 39: Cylinder: General (Geometry).	57
Figure 40: Simulation Control: General Species Setup (Gasoline/Default).	58
Figure 41: Simulation Control: General Species Setup - Initialization (Gasoline/Default).	58
Figure 42: System Boundary Condition for the intake (SB1) (Gasoline/Default).	59
Figure 43: System Boundary Condition for the exhaust (SB2) (Gasoline/Default).....	59
Figure 44: Injector: General data (Gasoline/Default).	60
Figure 45: Injector: Mass Flow Specification (Gasoline/Default).	60
Figure 46: Catalyst: General (Gasoline/Default).....	61
Figure 47: Catalyst: Type Specification (Gasoline/Default).	61
Figure 48: Catalyst: Friction (Gasoline/Default).	61
Figure 49: Cylinder: Initialization (Gasoline/Default).	62
Figure 50: Cylinder: Combustion model (Gasoline/Default).	62
Figure 51: Cylinder: Vibe (Gasoline/Default).	62
Figure 52: Simulation Control: General Species Setup (H ₂).	63
Figure 53: Simulation Control: General Species Setup - Initialization (H ₂).	63
Figure 54: System Boundary Condition for the intake (SB1) (H ₂).....	64
Figure 55: System Boundary Condition for the exhaust (SB1) (H ₂).	64
Figure 56: Cylinder: Initialization (H ₂).	65
Figure 57: Cylinder: Pollutants (H ₂).	65
Figure 58: TC: Compressor (H ₂).....	66
Figure 59: TC: Turbine (H ₂)	66
Figure 60: Air Cooler: General (Geometry) (H ₂).....	67
Figure 61: Air Cooler: Reference Operating Conditions (H ₂).....	67
Figure 62: Comparation of the fitting curve and the data of 2000rpm and Lambda 3.4, considering every point of the data.	69
Figure 63: Comparation of the fitting curve and the data of 2000rpm and Lambda 3.4, without data above 756.6 CA.	69
Figure 64: Graphical summary of the linear correlations between Parameter a and Combustion duration from fitting parameter at 2000 rpm and different lambdas.	70
Figure 65: Graphical summary of the linear correlations between Parameter a and Combustion duration from fitting parameter at 3000 rpm and different lambdas.	71

Index of Tables

Table 1: Comparison of Hydrogen properties against Methane, Gasoline and Diesel.....	13
Table 2: Gasoline Engine Results	38
Table 3: Main results of the simulations. Firstly, the results of the lean-burn approach are shown, and secondly, the results of CR reduction are shown.	42
Table 4: Global performance comparison between H2 ICE at 2000 rpm, Lambda = 2 and CR = 11.5 with and without TCI for different pressure boost	45
Table 5: Global performance comparison between H2 ICE at 2000 rpm, Lambda = 2 and CR = 9 with and without TCI for different pressure boost.	46
Table 6: Global performance comparison between H2 ICE at 2000 rpm, Lambda = 2.8 and CR = 11.5 with and without TCI for different pressure boost.	47
Table 7: Global performance comparison between H2 ICE at 3000 rpm, Lambda = 2.8 and CR = 11.5 with and without TCI for different pressure boost.	47
Table 8: Summary of the simulations with the combination of the approaches with CR = 9 and Lambda taking values of 2.8, 3.4 and 3.5	49
Table 9: Summary of NOx emissions for the set simulation of combination of approaches.	50
Table 10: The best results from the fitting script for the vibe function, from which correlations are extracted.	69
Table 11: Set 1: Efficiencies (Lean-burn approach).	0
Table 12: Set 1: Performance (Lean-burn approach).	1
Table 13: Set 1: NOx Emissions (Lean-burn approach).	2
Table 14: General Gasoline engine Results.	3
Table 15: Set 2: Efficiencies (Compression Ratio Reduction).....	4
Table 16: Set 2: Performance (CRR).....	5
Table 17: Set 2: NOx Emissions (CRR)	6
Table 18: Set 3: Efficiencies (TCI)	7
Table 19: Set 3: Performance (TCI)	8
Table 20: Set 3: NOx Emissions (TCI)	9
Table 21: Set 4: Efficiencies (TCI + CRR)	10
Table 22: Set 4: Performance (TCI + CRR).	11
Table 23: Set 4: NOx Emissions (TCI + CRR).	12
Table 24: Set 5: Efficiencies (TCI + Lean-burn).	13
Table 25: Set 5: Performance (TCI + Lean-burn).	14
Table 26: Set 5: NOx Emissions (TCI + Lean-burn).....	15
Table 27: Set 6: Efficiencies (TCI+CRR+Lean burn $\lambda = 2.8$).	16
Table 28: Set 6: Performance (TCI+CRR+Lean burn $\lambda = 2.8$).	17
Table 29 Set 6: NOx Emissions (TCI+CRR+Lean burn $\lambda = 2.8$).	18
Table 30: Set 6: Efficiencies (TCI+CRR+Lean burn $\lambda = 3.4$).	19
Table 31: Set 6: Performance (TCI+CRR+Lean burn $\lambda = 3.4$)	20
Table 32: Set 6: NOx Emissions (TCI+CRR+Lean burn $\lambda = 3.4$).	21

1. Introduction.

1.1. Background.

Since the Industrial Revolution, there have been incredible inventions and discoveries in both sciences and engineering at every level. Humans have made big advantages to help themselves in daily life activities such as transportation inventions (trains, cars, motorcycles, planes, etc.) or in getting better and faster production chains.

In different parts of the world, there were countries that developed huge industries; meanwhile, in other parts of the world, there were countries that still were years apart from the levels of industrialisation and production of these leading countries. After having different crises in the early 20th century all over the world; the world began to be more connected between countries, culturally and economically, also allowed companies to exchange different types of resources and products, even create holdings of companies from different sectors of the industry which ease the improvement of production and productivity.

Although on one hand, this phenomenon has some advantages, on the other hand, it has led the world to an age of careless consumption of new products without considering how these methods of production and products could affect the environment, and how much damage was doing it.

For several years now, the world has been facing a global warming period, contamination, and careless consumption. Global organisations and countries are concerned about these statements and how harmful can be to human health and future lives. In addition to these new challenges, there are others that were already present and have been exacerbated and become more relevant (No poverty, zero hunger, affordable and clean energy, sustainable cities and communities...). Owing to this the United Nations (UN) created in 2015 the Agenda 2030 for Sustainable Development with 17 Goals with strategies to promote prosperity while protecting the planet [11].

For sustainable transportation, the greenhouse gases, the microparticulate, the unburned particles of the fuel, and the nitrox-oxide (NO_x) created during the combustion process must be reduced to low levels and in the end, eliminate to achieve net zero by 2050.

Due to regulations about pollution, the use of the most established fuels Gasoline and Diesel have to be reduced in a highly manner in order to increase sustainable mobility.

According to UN infographic 13: climate change [23] it is needed to improve air quality in European countries and “reduce the greenhouse gases emissions by 43% by 2030 and to net zero by 2050”. These concerns about air quality led the European Union to the creation and implementation of the Euro standard regulation, under which new vehicles had to comply with requirements limiting gases potentially hazardous to health.

“For passenger cars and vans, the current Euro 6 test conditions and exhaust emissions limits will be maintained. For buses and trucks, stricter limits will be applied for exhaust emissions measured in laboratories and in real driving conditions, while maintaining the current Euro VI testing conditions.” [9]

These regulations provide a good context to implement new ways of sustainable mobility apart from improving the technology we already have, based on fossil fuel. Some alternative fuels have been developed as [3]:

- Biofuels.
- Synthetic and paraffinic fuels.
- Natural gas including biomethane, in gaseous form (compressed natural gas, CNG).
- Liquefied Natural gas (LNG).
- Liquefied petroleum gas (LPG).
- Hydrogen.

But also, there have been developments in the electric field:

- Electric vehicles (EV).
- Hybrid vehicles (HEV) and plug-in Hybrid vehicles (PHEV).
- Fuel cell.

Hydrogen is one of the most suitable fuels because, from the point of view of pollutants, hydrogen does not generate CO₂ and CO or unburned particles from its combustion. However, it can produce NO_x, these types of pollutants are one of the big problems of hydrogen internal combustion engines [27].

The aim of this project is to analyse different approaches and combinations of them in order to obtain a low or nearly zero NO_x emissions the Hydrogen internal combustion engine could have, with a level of efficiency near the current engine in use. This is going to be achieved by the implementation of an internal combustion engine model prepared for hydrogen fuel in AVL BOOST™.

1.2. Assumptions and constraints.

The combustion reaction of hydrogen would not create gases as CO₂ or pollutant as CO or any kind of particles or hydrocarbon from the combustion. This happens due to the absence of carbon into the reaction between the fuel and the air where the main important pollutant to be consider is NO_x [1,6,19,24-27].

The model will be chosen from an example in the program AVL BOOST™ and adapted to the requirements of a hydrogen ICE. The simulation of the model will be done with the same program.

The simulation control will be set up with the General Species Transport approach in order to obtain the composition of the exhaust gases.

For simplicity, blow-by rates have been set to zero for this work.

1.3. Scope of the work.

This diploma work will consist of seven chapters beginning with this first introductory chapter. Followed by the second chapter, which discusses the properties of hydrogen and the considerations that need to be taken into account when using it as a fuel. Moreover, a common and simple colour classification according to the hydrogen production process will be explained.

Next, in the third chapter the methodology followed to build the model and find a proper combustion model in AVL BOOST™ will be explained.

Afterwards, In the fourth chapter the various cases of the simulation will be set. And different strategies to reduce the NO_x emissions will be discussed and implemented.

In chapter five the results of emissions and efficiency parameters will be presented and compared to gasoline engine results.

Finally in chapter six the results will be discussed and general conclusions about the work and hydrogen-fuel internal combustion engines will be presented in chapter seven.

2. Hydrogen

After understanding the environmental problem and before starting the study of the different approaches, it is important to settle down some ideas about the hydrogen as energy carrier. This means is a substance that can be storage, to later be transformed in some other kind of energy.

2.1. Properties of the hydrogen

Hydrogen is the lightest and most abundant chemical element in the universe, making up 75% of the matter in the universe [14]. It is represented by the symbol H and atomic number 1. It is the first element on the periodic table and is commonly found in diatomic form as H₂. At room temperature, hydrogen is a colourless, odourless, non-metallic, and highly flammable gas. Its structural simplicity, with a single proton and a single electron, gives it unique properties that make it particularly relevant for energy applications, such as combustion in engines. Some of these important properties of internal combustion engines are described below based on Stępień [19] and Verhelst and Wallner [27].

At atmospheric pressure and a temperature of 273 K, hydrogen exhibits a significantly lower density than natural gas, primarily due to its **low molecular weight** (2.016 g/mol) [19,27]. This results in hydrogen having **the highest mass–energy ratio** among chemical fuels. In terms of mass–energy consumption, hydrogen surpasses conventional gasoline by approximately three times, alcohol by five to six times, and methane and propane by 2.5 times [19]. Consequently, blending hydrogen with hydrocarbon fuel can enhance engine efficiency and reduce specific fuel consumption [19].

However, the **low density of hydrogen** (0.089 kg/m³) leads to a **reduced energy density** of the hydrogen-air mixture within the engine cylinder, which in turn results in low power output [19,27]. A solution to this issue is the direct injection of hydrogen with the intake valve closed, which prevents the reduction in power output. To increase the hydrogen density and associated volumetric energy content, hydrogen storage pressure must be increased. For instance, compressing hydrogen to 350 bar at 273 K increases its density to 31 kg/m³, while the volumetric energy content rises to 3700 MJ/m³ [19].

The combustion process benefits from hydrogen's **high molecular diffusivity and flame speed**, which facilitate the rapid formation of a homogeneous fuel-air mixture and improve combustion efficiency and cycle-to-cycle variation within the cylinder [19,27].

Using gaseous fuel during engine start-up and warm-up avoids issues associated with the evaporation of cold liquid fuel and prevents uneven fuel distribution to the cylinders caused by liquid layers on the intake manifold walls. This helps maintain a consistent fuel-air mixture ratio during transitions like acceleration or deceleration [19].

Hydrogen's **wide flammability limits** (4 – 75 % compared to gasoline's 1.4 - 2.3 % by volume in air) allow it to operate on a lean mixture. These broad flammability limits from as poor as $\lambda = 10$ ($\Phi = 0.1$) to as rich as $\lambda = 0.14$ ($\Phi = 7$), this enables a wide range of engine power adjustments by varying the mixture composition [19, 27]. Moreover, unthrottled engine operation at partial loads, due to hydrogen's wide flammability range, improves thermal efficiency. The flammability limits expand with increasing temperature, lowering the lower flammability limit to 2 % volume at 300 °C ($\lambda = 20$, $\Phi = 0.05$) [19]. The upper flammability limit is pressure-dependent but less relevant for engine applications. Running on a lean mixture reduces flame temperature, thereby decreasing heat transfer to the walls and enhancing fuel economy by maximizing fuel combustion. This also results in lower NO_x emissions and increased brake thermal efficiency. However, overly lean mixtures can reduce power output due to the decreased volumetric heating value of the fuel-air mixture [19, 27].

The **minimum energy required to ignite** a hydrogen-air mixture at atmospheric conditions is remarkably low, about 0.017 mJ for hydrogen concentrations of 22-26% ($\lambda = 1.2-1.5$, $\Phi = 0.67-0.83$), much lower than the 0.24 mJ needed for a gasoline-air mixture [7, 19, 27]. This value is for a 0.5 mm spark plug gap, while a 2 mm gap requires approximately 0.05 mJ for hydrogen concentrations between 10% and 50% ($\lambda = 0.42-3.77$, $\Phi = 0.27-2.38$) [19, 27]. Below 10% hydrogen concentration, the ignition energy increases sharply, posing a risk of premature ignition from hot gases and hot spots in the combustion chamber. Due to its low ignition energy, a low-energy spark can ignite hydrogen, allowing the use of a glow plug or resistance hot wire [19]. Hydrogen's **small quenching distance** of 0.6 mm means the combustion flame is extinguished closer to the cylinder wall than with other fuels, impacting crevice combustion and heat transfer [19]. Hydrogen flames are difficult to extinguish, leading to backfire risks, especially through nearly closed intake valves. The quick burning of the hydrogen flame leads to increased lubricant evaporation and particle formation in direct injection hydrogen internal combustion engines (ICEs), but these traces of CO₂ and particulates are almost zero, so can be neglected [7, 19, 27].

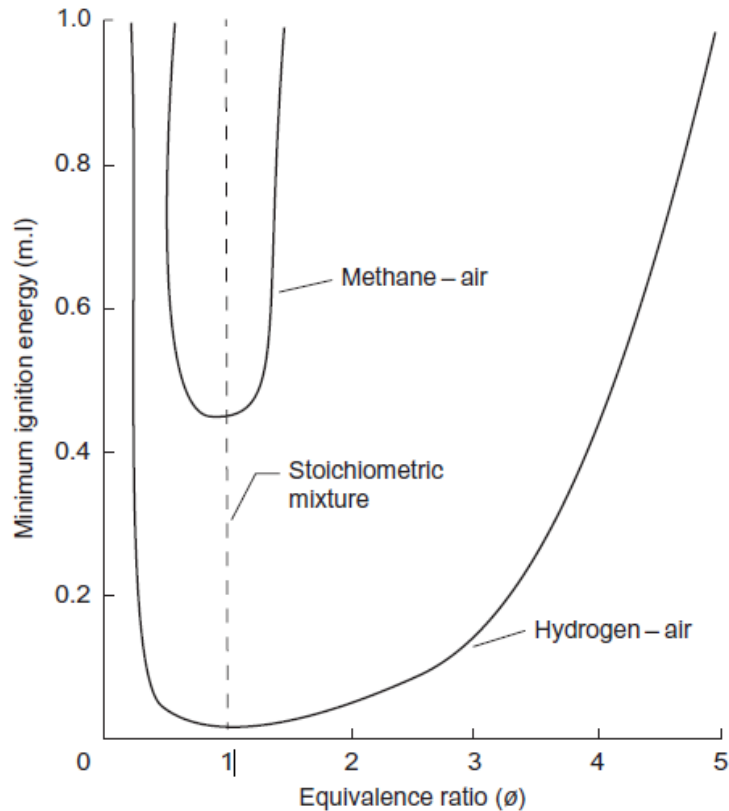


Figure 1: Minimum ignition energy for hydrogen and methane [7].

Hydrogen's **autoignition temperature** is around 853 K, much higher than that of other fuels, which complicates ignition only because of the temperature rise during compression [19, 27]. Thus, an **additional ignition source is necessary** for hydrogen-air mixtures. This high autoignition temperature allows for higher compression ratios in hydrogen-fuelled engines and reduces the risk of knocking combustion due to its high octane number [19]. However, the low minimum ignition energy increases the risk of premature, uncontrolled fuel ignition from hot spots, potentially leading to knocking combustion and mechanical damage to the engine [19]. The motor octane number (MON) of hydrogen is significantly lower than its research octane number (RON) compared to a typical drop of 8 to 10 points for gasoline, although the exact MON value is not clearly defined, because these methods were defined and prepared only for liquid spark ignited (SI) engine fuels [19, 27].

For the complete combustion of hydrogen in air, the **stoichiometric air-fuel (A/F) ratio** is 34.29 kg of air per 1 kg of hydrogen, corresponding to 29.52 % hydrogen in air by volume, much higher than the 14.7:1 A/F ratio for gasoline [19, 27]. Hydrogen's **high flame speed** at stoichiometric ratios allows hydrogen engines to approximate the

thermodynamically ideal engine cycle more closely. At leaner mixtures, flame velocity decreases significantly, improving fuel economy [19, 27]. The adiabatic flame temperature and velocity affect engine parameters such as thermal efficiency, combustion stability, and exhaust emissions [19]. Hydrogen's high diffusivity aids in forming a homogeneous fuel-air mixture and enhances safety by rapidly dispersing in case of leaks [7, 19, 27].

To summarize all these properties and compare them against other current fuels the following table 1 has been elaborated based on Stępień [19]:

Table 1: Comparison of Hydrogen properties against Methane, Gasoline and Diesel.

Properties	Hydrogen	Methane	Gasoline	Diesel
Carbon content [mass%]	0	75	84	86
Lower (net) heating value [MJ/kg]	120	45.8	43.9	42.5
Density (at 1 bar and 273 K) [kg/m ³]	0.089	0.72	730 - 780	830
Volumetric energy content (at 1 bar and 273 K) [MJ/m ³]	10.7	33.0	33 x 10 ³	35 x 10 ³
Molecular weight [g/mol]	2.016	16.043	≈110	≈170
Boiling point [K]	20	111	298 – 488	453 - 633
Auto-ignition temperature [K]	853	813	≈623	≈523
Stoichiometry air/fuel mass ratio	34.4	17.2	14.7	14.5
Minimum ignition energy in the air (at 1 bar and stoichiometry ratio) [mJ]	0.02	0.29	0.24	0.24
Quenching distance (at 1 bar, 298 K and stoichiometry ratio) [mm]	0.64	2.1	≈2	-
Laminar flame speed in air (at 1 bar, 298 K and stoichiometry ratio) [m/s]	1.85	0.38	0.37-0.43	0.37-0.43
Diffusion coefficient in air (at 1 bar and 273 K) [m ² /s]	8.5 x 10 ⁻⁶	1.9 x 10 ⁻⁶	-	-
Flammability limits in air [vol%]	4-76	5.3 - 15	1 - 7.6	0.6 - 5.5
Adiabatic flame temperature (at 1 bar, 298 K and stoichiometry ratio) [K]	2480	2214	2580	≈2300
Octane number (R+M)/2	130+	120+	86 – 94	-
Cetane number	-	-	13 – 17	40 – 55

2.2. Production processes and classification of hydrogen according to these processes

It is well known that hydrogen is the most abundant element in the universe. However, it cannot easily be found on Earth in isolation. Because it is always combined with other elements, it needs to be separated by some process in order to be used as a fuel.

Because hydrogen has to be separated from other elements, significant amounts of energy must be applied to produce it. There are several processes by which hydrogen can be obtained. Depending on the source of energy or the raw material from which hydrogen is obtained, it can affect the environment in different ways and can be classified as one colour or another.

In the following, the processes and classification of hydrogen in colours will be briefly explained:

2.2.1. From **non-renewable sources**: *black, brown, and grey.*

Brown/black hydrogen comes from coal gasification. If it is brown it comes from lignite (vegetable origin) and if it is black from bituminous coal. This is a process that is currently in disuse, except in China. [12].

Grey hydrogen comes from natural gas, methane, and LPG which during the reforming process convert them into hydrogen and release CO₂. This is the type of hydrogen that accounts for most of the production (approximately 95%) and one of the most polluting [12,14,18].

2.2.2. **Experimental hydrogen** (possible new sources): *orange, amber, white:*

Orange hydrogen is obtained by trying to take advantage of waste or emissions from other sectors to avoid negative environmental impacts, such as incinerating it or depositing it in a landfill. It is produced by converting biomass into hydrogen. In this case, the CO₂ emission is not captured, but it is used.

If the CO₂ is not only used but also captured and stored so that it does not reach the atmosphere, the **hydrogen will be amber**.

White hydrogen corresponds to hydrogen that is found directly in underground deposits in gaseous form. A resource that is little exploited due to its economic unviability and inefficient extraction techniques.

2.2.3. *Emission-free hydrogen: blue, pink (magenta) and green (renewable).*

The European Commission has proposed certain requirements for classifying hydrogen and its derivatives as renewable fuels. For hydrogen to be considered renewable, it must come from 90 % clean energy sources. On the other hand, for hydrogen to be considered low carbon if it comes from non-renewable energy sources, its lifetime greenhouse gas emissions must be less than 70 % of those emitted by natural gas. However, not all Eurozone countries consider low-carbon fuels as renewable energy sources.

Blue hydrogen occupies an intermediate position between non-renewable hydrogen and green hydrogen. It is produced from the reforming of natural gas, but the CO₂ generated in the process is captured to prevent its release into the atmosphere. In some cases, this CO₂ is stored in geological wells.

Another type of hydrogen is **pink or magenta hydrogen**, which is obtained by electrolysis or thermolysis (which can also be classified as **yellow hydrogen** [22] or red [21] using nuclear energy. This process does not emit harmful gases, so it is considered clean and emission-free energy, but it generates radioactive waste that is difficult to dispose of.

Of the diverse types of hydrogen, **green hydrogen** is the most sustainable and the one considered by all countries as **renewable**. It is obtained using renewable energies such as wind and solar power, using the excess energy for the electrolysis of water. The latter can also be considered as **yellow hydrogen** [4,21] if solar energy is used in order to create hydrogen via thermolysis. This process is clean and does not generate environmentally harmful waste. However, at present, green hydrogen production accounts for less than 1 % of the total hydrogen produced, according to the International Energy Agency (IEA). [12]

Below, some images show different colour classifications. Although they differ from each other in some colours, they all belong to official organisations or important companies in the sector. So, all of them can be taken into account, as long as it is specified which one is used.

	Colour	Fuel	Process	Products
	Brown/Black	Coal	Steam reforming or gasification	H ₂ + CO ₂ (released)
	White	N/A	Naturally occurring	H ₂
	Grey	Natural Gas	Steam reforming	H ₂ + CO ₂ (released)
	Blue	Natural Gas	Steam reforming	H ₂ + CO ₂ (% captured and stored)
	Turquoise	Natural Gas	Pyrolysis	H ₂ + C (solid)
	Red	Nuclear Power	Catalytic splitting	H ₂ + O ₂
	Purple/Pink	Nuclear Power	Electrolysis	H ₂ + O ₂
	Yellow	Solar Power	Electrolysis	H ₂ + O ₂
	Green	Renewable Electricity	Electrolysis	H ₂ + O ₂

Figure 2: Classification of Hydrogen in colours from the Sustainable NI blog [21].

Colors	Black Hydrogen	Grey Hydrogen	Blue Hydrogen	Turquoise Hydrogen	Yellow Hydrogen	Pink Hydrogen	Green Hydrogen
Process	Gasification	SMR	SMR or gasification with carbon capture (85-95%)	Pyrolysis	Sulfur-iodine cycle	Electrolysis	Electrolysis
Source	Coal	Methane	Methane or coal	Methane	Nuclear power	Nuclear power	Renewable Energy

Figure 3: Simplified classification of hydrogen colours from the United Nations Economic Commission for Europe Committee on Sustainable Energy (UNECE) [22].

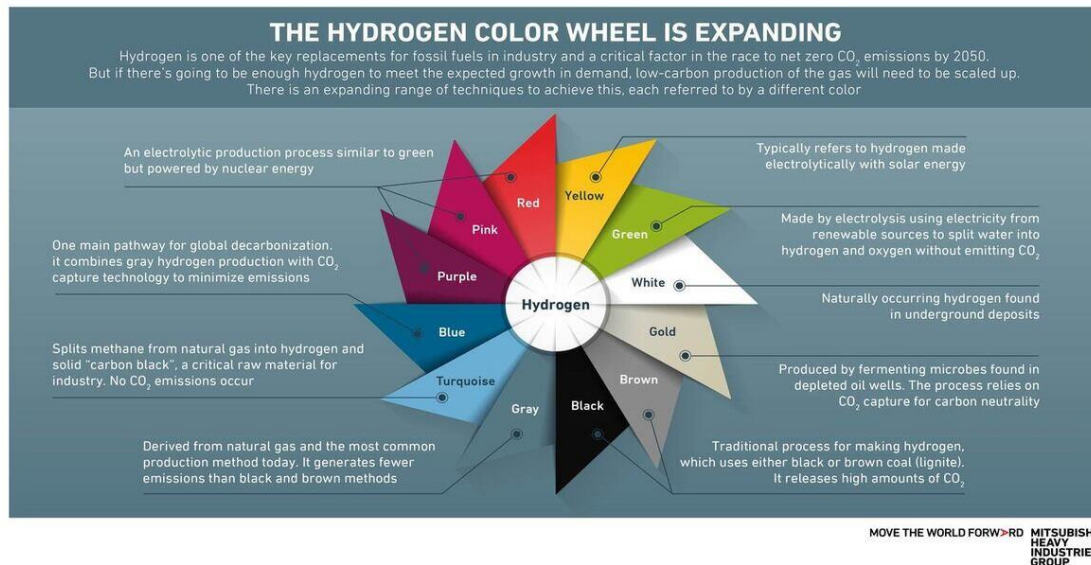


Figure 4: The Hydrogen colour wheel by Mitsubishi Heavy Industries Group [4].

Following the guidelines of obtaining a planet with zero emissions, green hydrogen is presented as a clean and renewable energy alternative. But in addition, this method also comes with other advantages [5], such as:

Efficiency in water consumption. To produce 1 kg of hydrogen by electrolysis, 10 litres of deionized water are required, by natural gas reforming with CO₂ capture 25 litres are necessary and if it is by natural gas reforming, but without CO₂ capture, 23.5 litres are needed.

This shows that electrolysis is the most efficient method in terms of water consumption, one of the essential resources along with renewable electricity.

Although, in economic terms, blue hydrogen has a lower initial cost due to the use of hydrocarbons. However, this method includes CO₂ capture and storage, which implies additional costs. Similarly, magenta hydrogen, despite being obtained in nuclear power plants through the hydrolysis of water, ends up generating radioactive waste that is difficult to dispose of [12]. In addition, the plants that have already been amortized are usually far from industries that need this energy [13]. Nonetheless, with technological advancement and the construction of new green hydrogen plants, costs are expected to gradually decrease, narrowing the gap with blue hydrogen [5].

Finally, considering the country's capacity to obtain renewable sources of natural resources. Green hydrogen strategically limits or eliminates dependence on third countries [5].

2.3. Ways of storage the hydrogen and its safety.

Due to the low density of hydrogen, big tanks are needed to store an adequate amount of energy and to obtain a good range. Therefore, for the use of hydrogen as a transport fuel, it will be necessary to store it in a compressed liquid or cryogenic state to reduce storage volumes; however, there are research and development in solid state storages, attaching the Hydrogen to other chemical substances via reversible metallic hydride formation reactions (this last type of storage is expensive and need special infrastructure) [10]. Considering the big volume required for storage enough hydrogen, it is more likely to see the focus of such engines in heavy-duty vehicles. However, as technology improves, tanks may become smaller or even rechargeable with internal water electrolysis systems, and light duty vehicles without big tanks will be possible. Different ways of hydrogen storage are currently being developed and are described briefly below [10, 14, 15].

- Compressed Gas
- Liquid/cryogenic Hydrogen
- Chemical hydride
- Metallic hydride
- Nanocarbon tubes

Compressed Gas: Storing hydrogen in its gaseous state involves compression to high pressures. Only relatively small amounts of hydrogen are stored at 200 bar, thus, typically values of storage are between 350 to 700 bar. This method necessitates robust and durable storage tanks made from advanced materials to withstand the high pressure; however, high pressure storage (700 bar) is still under development [14, 15]. The design and construction of these tanks are critical to prevent leaks and ensure safety.

Liquid hydrogen: This storage requires cryogenic temperatures below 20 K. This method is more energy-intensive due to the cooling processes involved. Additionally, specialized insulated containers are necessary to maintain these extremely low temperatures and minimize boil-off losses [10].

Solid Hydrogen: Hydrogen can also be stored in solid forms such as metal hydrides, chemical hydrides, and adsorption materials. These methods offer the advantage of higher energy densities and lower pressures compared to gaseous storage. However, they require further research and development to improve their efficiency, reversibility, and cost-effectiveness [10, 14].

Concerning safety, it is important to consider the fact that hydrogen ignites easily, even with minor energy sources like electrostatic sparks. Fires from hydrogen burn rapidly, leading to short-lived flames. What can have pros and cons, because as it can be seen later the fires last less than gasoline fires, but it can cause fatal explosions if the fire backflow to the tank. Hence, ensuring material compatibility, particularly regarding hydrogen embrittlement, and evaluating components for strength, hardness, and machinability are crucial. Steel has low permeability to hydrogen at room temperature but a high diffusion coefficient, needing the use of flame arrestors in hydrogen systems to prevent explosions. Leak detection is vital, with sensors installed to monitor hydrogen levels, particularly as concentrations approaching 4% by volume are flammable [7].

Extensive research by Dr. M.R. Swain at the University of Miami shows that, with proper handling, hydrogen can be safer than gasoline. Figure 5 “clearly demonstrates that hydrogen could be safer than gasoline if properly handled.” [7].



Figure 5: Demonstration of hydrogen safety: hydrogen fire (left) versus gasoline fire (right) [7]

This photo extract from Das [7] is part of a video from a research of Dr. Michael Swain (University of Miami), where it is possible to compare an intentional hydrogen tank release and a small gasoline fuel line leak. After 60 seconds, the hydrogen flame begins to ease, while the gasoline fire intensifies. After 100 seconds, all the hydrogen flame was extinguished, and the interior of the car was undamaged (the maximum temperature inside the rear window was 19.44 °C) [7]. “The gasoline car continued to burn for several minutes and was completely destroyed.” [7].

3. Abnormal combustion problems to avoid in a H₂ICE.

There are several abnormal combustion challenges that hydrogen-fuel internal combustion engines are prone to face. The main problem found in the development of

hydrogen engines is **premature ignition (pre-ignition)**. As a result, the engine behaviour starts to be erratic and inefficient, which causes the loss of maximum power. Premature ignition near the intake valve can cause **backfire**, which is when the flame travels back into the induction system. Backfire usually can happen when hot spots or hot exhaust gases ignite the hydrogen-air mixture entering the combustion chamber when the intake valves are opened, leading to flame retraction and/or uncontrolled combustion during the compression stroke. The only difference is the moment at which it happens.

Backfire is particularly problematic in Port Fuel Injection Hydrogen Internal Combustion Engines (PFI-H₂ICE), where hydrogen is mixed with air in the intake manifold before entering the combustion chamber. The combustible mixture in the manifold increases the likelihood of backfire, which can damage the intake system. This irregular and atypical combustion situation may occur in H₂ICEs because of hydrogen's wide flammability limits and low ignition energy helped by the high speed of flame propagation and low quenching distance.

In general, there are **three regimes of abnormal combustion** in spark ignition engines [19]:

1. **Knock combustion**, which is the term used in typical SI engines referring to spontaneous ignition of the remaining final gas during the late part of the combustion event, causing high-pressure waves.
2. **Pre-ignition** is the uncontrolled ignition from an external source of energy such as hot spots or final gases from the combustion.
3. **Backfire**, which is the premature ignition during the suction stroke. Which can be seen as a particular early form of pre-ignition.

Overall, hydrogen's wide flammability limits and low ignition energy, aided by the high speed of flame propagation and low quenching distance contribute to the complexities of abnormal combustion in hydrogen-fuelled ICE. In addition, pre-ignition is more likely to occur when hydrogen-air mixtures approach stoichiometric levels.

Limiting the maximum fuel-to-air equivalence ratio is an effective measure to prevent abnormal combustion in hydrogen fuelled engines. Hydrogen internal combustion engines typically employ a lean combustion strategy due to the wide flammability limits of hydrogen and fast flame speeds, thus avoiding choke losses. In lean operation, excess air functions as an inert gas, effectively reducing combustion and component temperatures [19,27]. This strategy significantly decreases the occurrence of abnormal combustion in lean combustion regimes [27]. Despite the efficiency of lean operation, it limits the power output of hydrogen engines. Furthermore, the choice of the injection system is crucial to avoid backfiring [19].

4. Justification of engine base line used.

First, hydrogen as fuel can be used in spark ignited (SI) as well as compression ignited (CI) engines [19]. The main problem with the CI engines for the case of study that is concerned in this work, is that hydrogen's high autoignition temperature implies high pressures which cannot be achieved in the cylinder. Hence, some element is needed to trigger the hydrogen combustion reaction. It can be spark plug, a glow plug or another fuel that has low autoignition temperatures. This is the reason there are many investigations about dual-fuel engines, where they focus especially in blends of hydrogen with other fuels. However, the presence of a fuel with Carbon in its formula makes that at the end of the combustion there were carbon oxides, unburned particles, and other pollutants. For this case of study, the aim is to reduce the emissions and especially NO_x . Therefore, to use hydrogen as standalone fuel, assuming that its combustion only creates nitrogen oxides, a spark ignition engine is used as base line.

5. Justification of induction technique used.

Lean burn air-fuel mixtures are the main approach we are going to follow in this study to reduce the emissions of Hydrogen Fuelled ICE, with the benefit of avoiding abnormal combustion problems. In addition, if further experimental work is going to be made based on this study its recommended to minimize any possible hot spot in presence of ignitable mixtures. This can be achieved with optimal valve crossing and with variable valve timing to optimise the renewal of the charge into the cylinder, thus, avoiding the contact between exhaust gases and hydrogen, moreover, the new air can cooldown the walls and the tip of the spark plugs and injectors. Carefully controlled injection timing can avoid having backfiring and knocking [6,7,25,27]. Another way to reduce NO_x emissions is to introduce liquid water into the combustion chamber. It can also prevent knocking combustion and premature ignition when burning hydrogen [19].

In the pursuit of optimizing hydrogen-fuelled internal combustion engines, the choice of fuel injection method plays a key role. This allows avoiding significant problems such as abnormal combustion, low power, or high NO_x emissions [19]. The two primary methods are Port Fuel Injection (PFI) and Direct Injection (DI). While both have reasons to be implemented in H2ICE, DI presents several advantages that make it a better choice for hydrogen-fuelled engines.

Port Fuel Injection (PFI) involves injecting hydrogen fuel into the intake port by mechanically or electrically controlled injectors after the start of the inlet stroke. This method allows for precise control of injection timing and duration, particularly at high engine speeds where electronic injectors are preferred. During the intake stroke, hydrogen is injected into the manifold, and air is supplied separately to dilute the hot residual gases, reducing the combustion chamber's temperature [19]. However, PFI has inherent disadvantages that impact the engine's efficiency and performance. One is the displacement of the volume of air trap in the cylinder, preventing the engine to reach the maximum efficiency. This is due to the low volumetric density of hydrogen, and the preparation of the fuel and air mixture outside the combustion chamber, leading to less precise control over the combustion process. This can be seen more graphically in the figure 6 from Verhelst et al. [25].

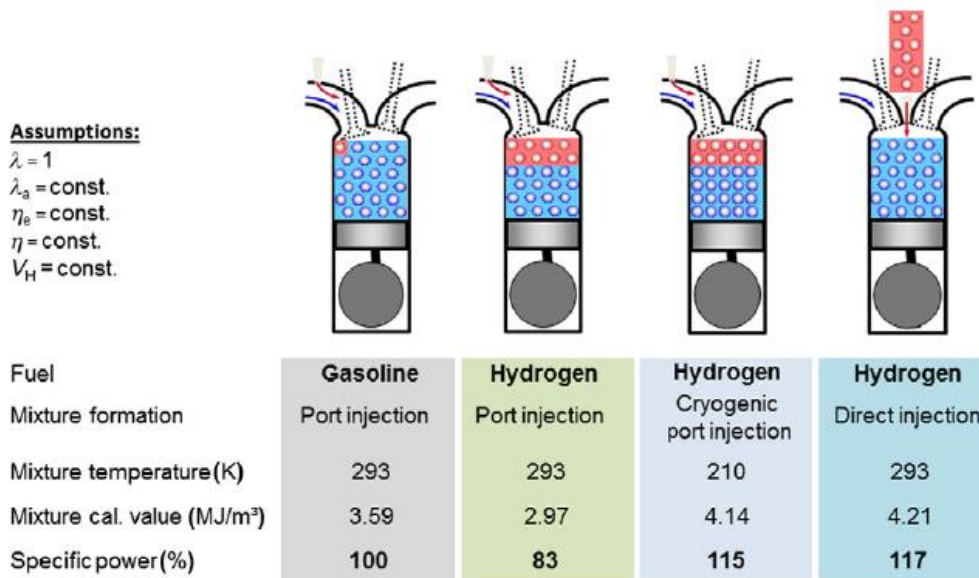


Figure 6: Comparison of specific power density of hydrogen mixture formation [25].

Another significant issue with PFI is the potential for backfire. Since hydrogen is a highly flammable gas, its mixture with air in the intake manifold can pre-ignite, causing backfire and posing a risk to engine components. [7,19,27].

On the other hand, Direct Injection (DI) offers several compelling advantages over PFI. DI systems inject hydrogen fuel directly into the combustion chamber at high pressures (200–300 bar), allowing for better control of the fuel-air mixture and the timing of combustion. This method significantly improves thermal and volumetric efficiency and allows for higher compression ratios. The precise control of different strategies of the

injection process in DI could eliminates the risk of backfire and knocking, enhancing the engine's reliability and performance [19].

It is possible to differentiate between two types of DI the high-pressure direct injection based on injecting the fuel at the end of the compression stroke, whereas the low-pressure direct injection system operates to inject the fuel after the closing of the intake valve, and under low cylinder pressures.

The high-pressure injection in DI enables diffusive combustion, avoiding preignition and knocking issues while increasing efficiency and power density. The premixed low-pressure DI combustion process represents a balanced compromise between efficiency, power density, raw emissions, and cost considerations [19].

In conclusion, Direct Injection (DI) stands out as the optimal fuel injection method for hydrogen-fuelled internal combustion engines. Its ability to enhance the power density, and thus, the thermal and volumetric efficiency for the same lean mixture than PFI. Besides, DI eliminate backfire and knocking risks, which are common in PFI. Although DI can create more NO_x emissions than PFI, the improve in safety and efficiency is worth enough to adopt direct injection as the induction technique.

6. Methodology

6.1. Introduction to the program AVL BOOST™ and its parts.

The analysis of the hydrogen combustion and its emissions is conducted using AVL BOOST™. BOOST™ is a program from AVL List GmbH (AVL), which is widely used in both the automotive and nonautomotive industries for engine cycle and gas exchange one-dimensional simulations. A wide range of engine speeds and sizes, including two-stroke and four-stroke engines can be modelled in the program.

The BOOST™ package consists of an intuitive Graphical User Interface pre-processing program through which the user introduces the input data for all available elements in the main calculation program. In the figure 7 is shown the main window with the model “4t1calc.bwf” from the examples of the program.

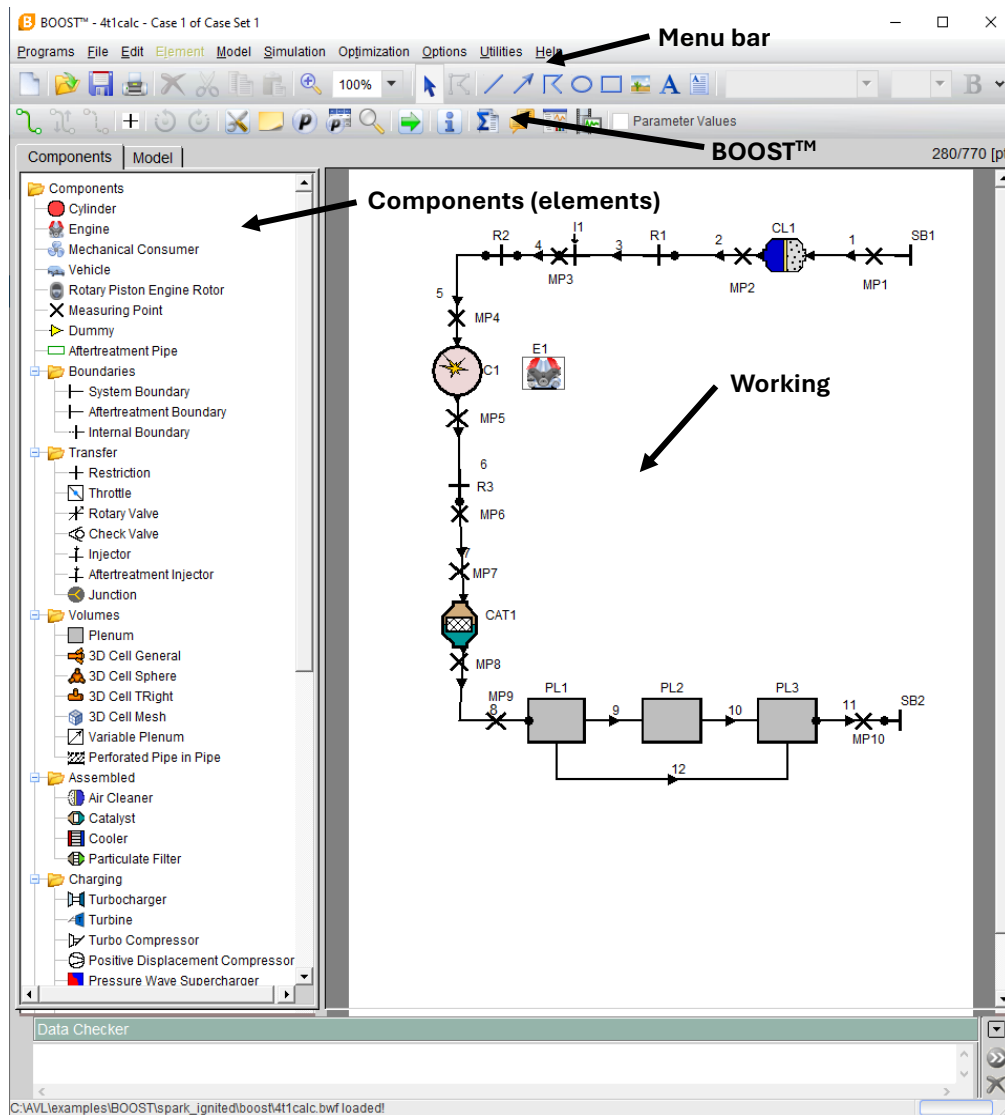


Figure 7: Explanation of the main window with a model from examples.

The main program provides optimised simulation algorithms for all available elements. According to BOOST™ User Manual and Theory documentation. The flow in the pipes is treated as one-dimensional. This means values of the physical parameters obtained from the solution of the gas dynamic equations, represent mean values over the cross-section of the pipes. Flow losses due to three-dimensional effects, at specific locations in the engine, are considered by appropriate flow coefficients.

Results analysis is supported by an interactive post-processor. Moreover, animated presentation of selected calculation results is available. Furthermore, individual curve results can be export in .csv files which allow to use them in another program if it is needed.

6.2. Justification of elected type of ICE

To simplify the building of the model. It was decided to start from an example model of Spark Ignited engines *4t1calc_species.bwf* because it already had implemented the general species approach. The flow coefficient and the values for the pipes and Air Cleaner have not been change. However, the initialization set have been updated to the values needed for the hydrogen fuel. In the Annex A figures 53, 54 and 55 show of the initialization global set up and the boundary conditions.

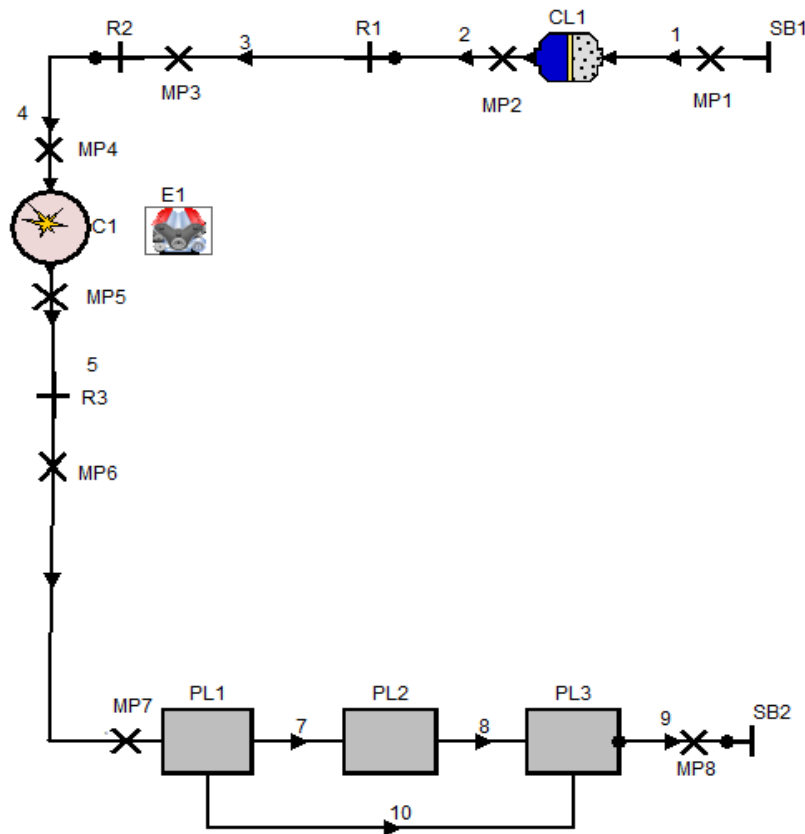


Figure 8: Basic model used for the simulations. It is based on figure 7 model.

Because of the selected induction technique, the Injector has been eliminated and the mixture preparation inside the cylinder element changed from External to Internal; the length of this pipe was adjusted to the previous length of this section.

Similarly, for the cases where the catalyst is not going to be used because the aimed result is to obtain near zero NO_x emissions, the catalyst is eliminated, and the length of the pipe was adjusted to the previous length of this section.

6.3. Choice of the combustion model used in the simulation.

After reading the theoretical documentation provided in the programme and researching for a better understanding of the possible combustion models that could best suit the behaviour of hydrogen, we proceeded to test the following models: Vibe (single zone, double zone, etc.), Fractals, AVL Mixing Controlled Combustion and AVL Multi-zone Combustion Model.

The last two are only enabled for the internal mixture preparation option (which would be equivalent to DI), but they are designed for compression ignition engines. Therefore, for the case of this study it would not be useful because it was decided to use a spark plug or glow plug to initiate combustion, in order to avoid the use of diesel which would add pollutant emissions. On the other hand, the Fractal-based combustion model can only be selected for external mixture preparations.

6.3.1. Vibe function / Wiebe function.

Since it is desired to have the flexibility to be able to analyse data with direct injection and ignition triggered configurations, the model that allows us to do these configurations, while keeping in mind the objective of analysing emission trends, is the Vibe law approach. This model is based on defining the parameters of the Vibe or Wiebe function. This approach starts from predefining the rate of heat released (ROHR) with the Vibe function, rather than having a model predict it. The combustion can be set with one, two or multiple functions, considering whether part of the premixed mixture is present and starts combustion and then gives way to diffusion-controlled combustion. There is also the concept of Vibe two zones, where the assumption that the zones of the burned and unburned charges have same temperatures is no longer followed. Instead, the first law is applied to the burned and unburned charges.

$$\frac{dx}{d\alpha} = \frac{a}{\Delta\alpha_c} * (m + 1) * \left(\frac{\alpha - \alpha_0}{\Delta\alpha_c}\right)^m e^{-a * \left(\frac{\alpha - \alpha_0}{\Delta\alpha_c}\right)^{(m+1)}} \quad (1)$$

$$dx = \frac{dQ}{Q} \quad (2)$$

This model requires the user to define the following parameters: α_0 , the start of combustion; $\Delta\alpha_c$, the duration of combustion; the shape parameter (m) and the parameter a (i.e. a = 6.9 for complete combustion) (BOOST™ Theory).

The integration of the vibe function results into the fraction of fuel mass which was burn since the start of the combustion process.

$$x = \int \frac{dx}{d\alpha} d\alpha = 1 - e^{-a * \left(\frac{\alpha - \alpha_0}{\Delta\alpha_c}\right)^{(m+1)}} \quad (3)$$

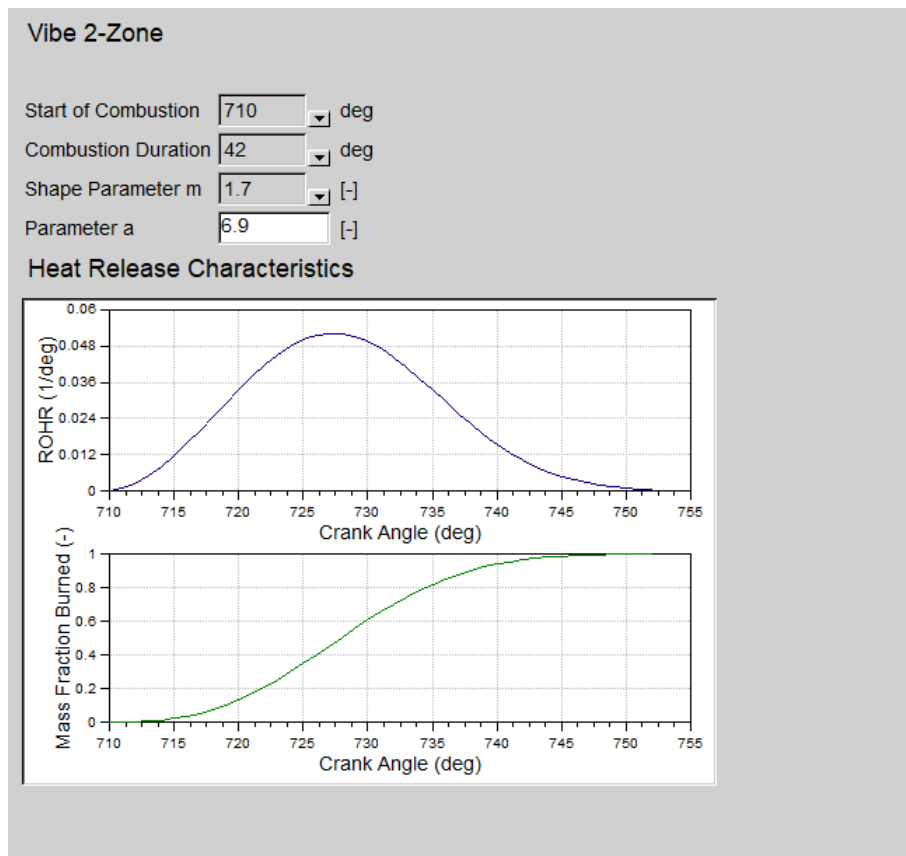


Figure 9: Vibe 2-zone section in the menu of combustion inside the cylinder element.

In this analysis study the vibe approached has been followed through the Vibe 2-zone, because it can be more accurate and allows to see the NOx emissions directly calculated by the simulation, where BOOST™ calculate them based on technical paper MTZ 34 1973 (12).

6.4. Analysis of in-cylinder pressure.

For this work, it was not possible to have access to a hydrogen engine to fit a combustion model or to measure the necessary parameters for the predictive combustion models in the programme. The vibe law parameters have been derived based on the experimental work already conducted in Verhelst and Sierens [26] and Sementa et al. [17].

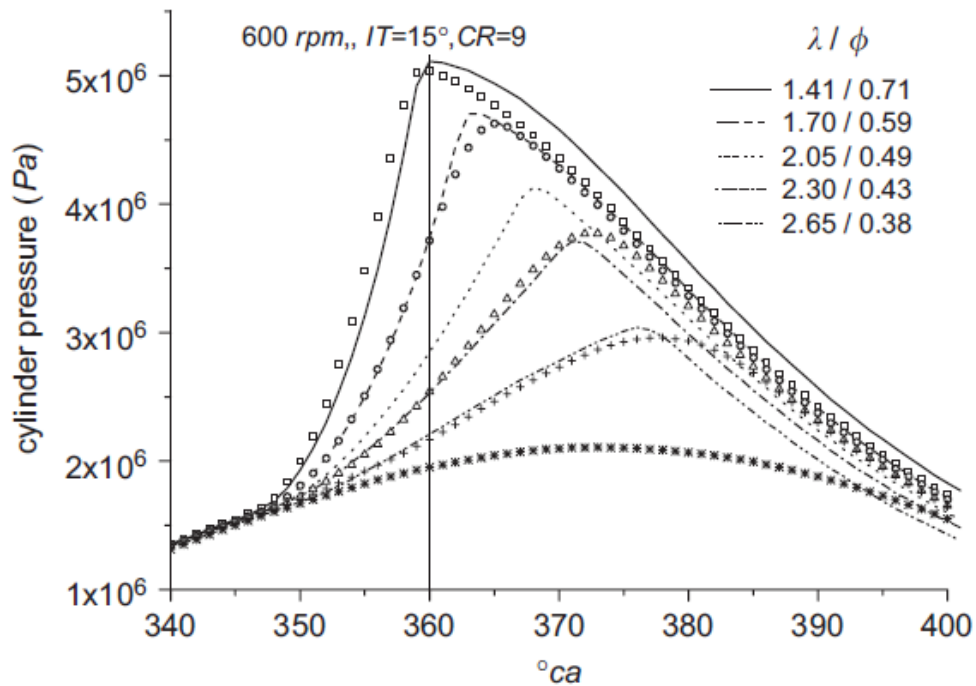


Figure 10: Results of in-cylinder pressure for different lambdas. The marks are the experimental values from S. Verhelst and Sierens [26].

Using the pressure curve, the fuel heat release rate is modelled by analysing the cylinder pressure history (with the combustion target pressure curve section within the Cylinder element). In this case, only the combustion part of the pressure curve was available, which caused problems with the simulation as it did not have pressure values at all points of the cycle. Therefore, an attempt was made to configure a pressure curve with the hydrogen values and completing the curve based on the pressure curve of the example with petrol from which it started.

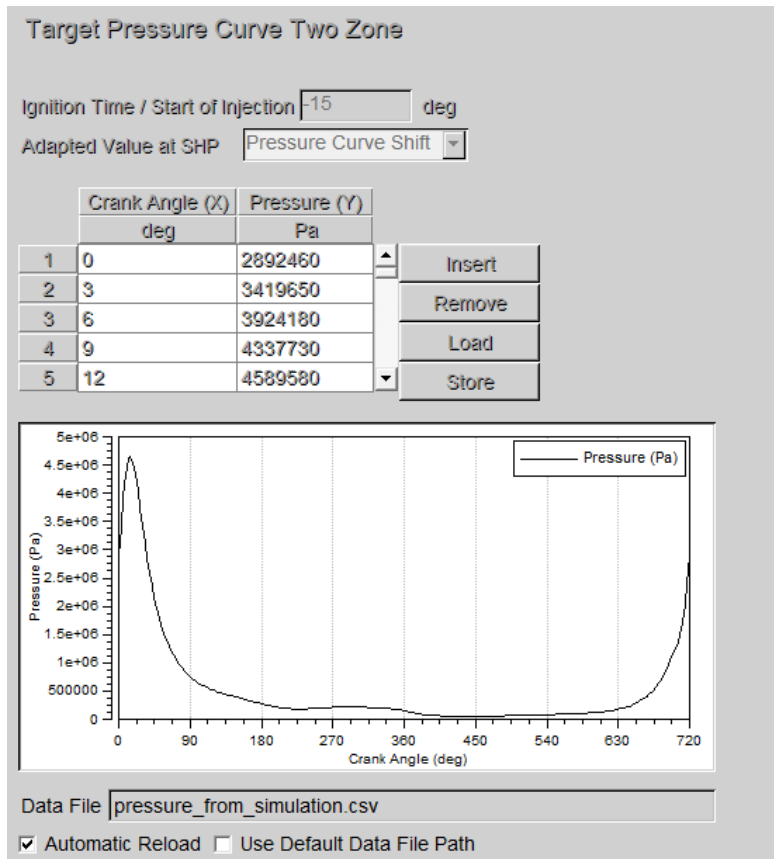


Figure 11: Target Pressure Curve two-zone combustion model menu inside cylinder element.

Subsequently, the results of the analysis provide us with a ROHR curve that will be exported in .csv format and the vibe law parameters that best fit the curve extracted from the simulation will be extracted. As an example:

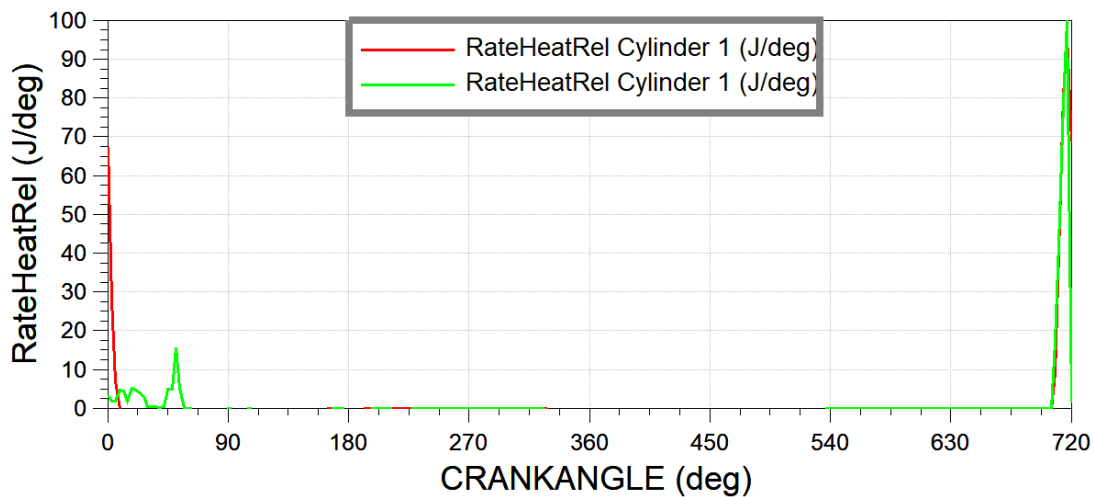


Figure 12: Comparison of Reat of Heat Release between Excel estimation in red and pressure analysis results in green.

The red one is the curve configured with the parameters found by trial and error in excel: 705 CA for start of combustion, 33 CA duration of the combustion, 1.7 for shape

parameter, and 6.9 for parameter a. While the green one is the curve provided by the simulation of the pressure analysis in the cylinder.

All this with the aim of having the parameters of a vibe law for different lambdas on an experimental basis based on hydrogen fuel.

6.4.1. ROHR of Hydrogen from literature

As previously mentioned, the article from Sementa et al. [17] was found to provide heat release rate curves at other engine speeds. This skips the pressure-analysis part of the simulation, speeding up the process of obtaining a fit to the vibe function. In addition, it opens the door to finding a correlation that allows the study to be extended and improved.

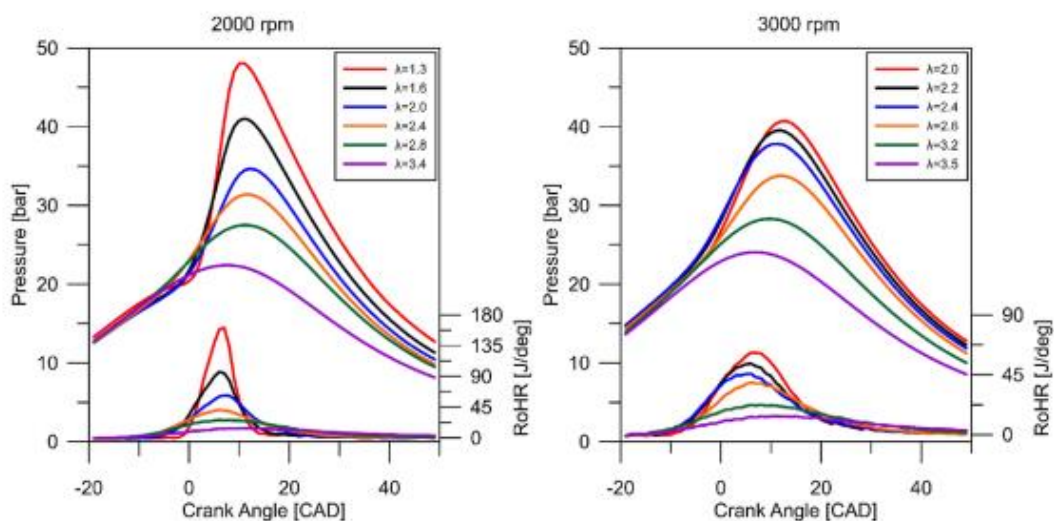


Figure 13: In-cylinder pressure and ROHR at different lambdas for engine speeds of 2000 rpm (left) and 3000 rpm (right) [17].

6.5. Curve fitting.

Since the fit with Excel did not allow to have an approximation that reflects well the ROHR, it was decided to start the development of a MATLAB script to fit the experimental data to the vibe function, by varying the parameters of our choice. This will be achieved through the **fit** function and the definition of the vibe function and its parameters within the **fittype** function. In addition, a number of options will be introduced to help the model obtain a better fit and find as few errors as possible.

```

1 A=table2array(readtable('ROHR_2000rpm_Lambda1-3.csv',Range="A3:B45"));
2 Angle = A(:,1);
3 Sample = A(:,2);
4
5 %%
6 Lambda = 1.3;
7 LambdaStoch = 34.3;
8 RatioAF = Lambda*LambdaStoch;
9 P = 1; %bar
10 V = 0.5; %L
11 R = 0.0821; %J/mol/K
12 T = 298; %K
13 mAir = (P*V)/(R/29*T); %g
14 mH2 = mAir/RatioAF; %g
15 LHV = 120000; %J/g
16
17 Q = mH2*LHV
18
19 %%
20 % Coefficient Lower Limits
21 a1=2;
22 b1=400;
23 CDl=5;
24 ITl=700;
25 ml=0.1;
26
27 %%
28 % Coefficient Upper Limits
29 au=6.9;
30 bu=2000;
31 CDu=50;
32 ITu=720;
33 mu=11;
34
35 %%
36 % Fit limit
37 AngleLim = max(Angle);
38 %AngleLim = 756;

```

Figure 14: Fragment of the fitting script. Initialization

Following the lines in figure 14. The script starts by reading the data from the file in which the experimental data has been saved. Then the minimum and maximum values that the parameters can take are set. In this way, the search for the minimum of the function is limited to a more concise range. Within the vibe function, a coefficient “b” has been introduced, which is defined as the combustion efficiency per total heat used in combustion, this being the mass of fuel per lower calorific value as it can be seen in (4) where “b” multiplies (1), and (5) is the implementation of this equation in the function fittype. With this coefficient “b” the vibe function returns the absolute values of the heat release rate, so is possible to fit the curves from the analysis of in-cylinder pressure.

Below, the equations from absolute ROHR and the one define in the script of MATLAB are a shown:

$$\frac{dQ}{d\alpha} = b * \frac{dx}{d\alpha} = m_f \cdot LHV \cdot \eta_f \cdot \frac{dx}{d\alpha} \quad (4)$$

```
ft = fitype('heaviside(CA-IT)*b*(a/CD)*(m+1)*((CA-IT)/CD)^m*
exp(-a*((CA-IT)/CD)^(m+1))','dependent',{ 'y' }, 'independent',{ 'CA' },
'coefficients', {'a','b','CD','IT','m'});
```

 (5)

Nevertheless, it has also been necessary to limit the search for the fit only to the higher values of IT (ignition timing). that represents the start of the combustion. Because some values of the parameters make that the vibe function gets a singular point which tents to infinity before the IT angle. This was solved introducing the **function heaviside(CA-IT)** that forced all the values before IT angle to take the value of zero.

In this case, the fit function has the problem of being dependent of the starting point. Because it tends to find the nearest local minima. While what it is needed is the global minimum of the fit function. So, a loop of the fit function with random starting points has been implemented in order to scour the space to find the global minimum or at least one of the lower points near to global minimum value. The procedure is as follows, a first iteration is set out of the loop as the minimum values of the fit, the goodness of fit, and output information of the fit. The root mean square error (rmse) is extract from the goodness of fit and set as the minimum rmse (rmse_min). Then, inside the loop the rmse of the new iteration is compared to the previous rmse_min, if the new one is smaller the data is update and the iteration number and the value of rmse_min is displayed. At the end of the loop the parameter of the accurate fit achieve in this run is display and both, Sample and the Minfit vibe curve are plotted to see if the result is satisfactory.

In case the results are not satisfactory the run can be repeated with new lower and upper bounds or adding values known to the parameters of the function vibe. Every workable solution parameter and rmse was saved and the parameters were used in the simulations with the vibe model. After having enough data from all the experimental cases collected from the articles of Verhelst and Sierens [26] and Sementa et al. [17] a linear interpolation was made to study the reductions emission approaches.

```

37 %%
38 ft = fitype('heaviside(CA-IT)*b*(a/CD)^(m+1)*((CA-IT)/CD)^m*exp(-s*((CA-IT)/CD)^(m+1)); dependent',{y},'independent',{CA},'coefficients',{a,'b','CD','IT','m'});
39 [MinFit,MinGof,MinOutput] = fit(Angle,Sample,ft,'startPoint',[5,0,10,710,2],'Lower',[a1,b1,CD1,IT1,m1],'Upper',[au,bu,CDu,ITu,mu],'Exclude',Angle > AngleLim);
40 rmse_min=MinGof.rmse;
41 fprintf('It %d,\trmse=%1.12f\n',1,MinGof.rmse)
42 for i = 1:1000
43     ai=a1+(au-a1)*rand;
44     bi=b1+(bu-b1)*rand;
45     CDi=CD1+(CDu-CD1)*rand;
46     ITi=IT1+(ITu-IT1)*rand;
47     mi=m1+(mu-m1)*rand;
48     [fitobject,gof,output] = fit(Angle,Sample,ft,'startPoint',[a1,b1,CD1,IT1,m1],'Lower',[ai,bi,CDi,ITi,mi],'Upper',[au,bu,CDu,ITu,mu],'Exclude',Angle > AngleLim);
49
50
51     if rmse_min > gof.rmse
52         rmse_min = gof.rmse;
53         MinFit = fitobject;
54         MinGof = gof;
55         MinOutput = output;
56         fprintf('It %d,\trmse=%1.12f\n',i+1,MinGof.rmse)
57     end
58 end
59

```

Figure 15: Fragment of the fitting script. Where the loop is implemented for 1000 iteration to find a proper minimum.

Based on the results of the fit vib curve gathered in the annex B, linear correlation between parameter “a” and combustion duration have been calculated with the Excel. Below, it appears every correlation used:

For $\lambda = 1.3$ and 2000 rpm:

$$CD = 0.6920 \cdot a + 11.9631 \quad (6)$$

For $\lambda = 1.6$ and 2000 rpm:

$$CD = 0.9791 \cdot a + 19.1094 \quad (7)$$

For $\lambda = 2$ and 2000 rpm:

$$CD = 2.2560 \cdot a + 16.0806 \quad (8)$$

For $\lambda = 2.4$ and 2000 rpm:

$$CD = 4.0071 \cdot a + 16.0094 \quad (9)$$

For $\lambda = 2.8$ and 2000 rpm:

$$CD = 5.1294 \cdot a + 24.2432 \quad (10)$$

For $\lambda = 3.4$ and 2000 rpm:

$$CD = 10.7263 \cdot a + 25.1281 \quad (11)$$

(considering the fit for all the data)

$$CD = 6.2133 \cdot a + 27.1182 \quad (12)$$

(considering the fit without the data above 350 CA)

Figure 62 and figure 63 in the Annex B shows the difference between both fittings.

For $\lambda = 2$ and 3000 rpm:

$$CD = 2.9762 \cdot a + 18.7914 \quad (13)$$

For $\lambda = 2.2$ and 3000 rpm:

$$CD = 2.7702 \cdot a + 23.2054 \quad (14)$$

For $\lambda = 2.4$ and 3000 rpm:

$$CD = 4.5521 \cdot a + 17.9342 \quad (15)$$

For $\lambda = 2.8$ and 3000 rpm:

$$CD = 4.6275 \cdot a + 22.0258 \quad (16)$$

For $\lambda = 3.2$ and 3000 rpm:

$$CD = 6.1126 \cdot a + 34.3696 \quad (17)$$

For $\lambda = 3.5$ and 3000 rpm:

$$CD = 9.4671 \cdot a + 34.9574 \quad (18)$$

(considering the fit for all the data)

$$CD = 6.3967 \cdot a + 41.1474 \quad (19)$$

(considering the fit without the data above 356.6 CA)

The interpolation between the values of the **Parameter a** from the fitting script maintains the shape of the ROHR for different values of **a** with almost no appreciable error. However, in case the correlations are used to extrapolate, a small change in the shape of the curve can be seen if the values of **a** are quite far away from the ones given from the fitting script. Figure 16 shows an example, with the values obtained for $\lambda = 1.3$ at 2000 rpm the correlation has been used for the values of:

- $a = 5,675$, which is known, and the $CD = 15,890$ CA
- $a = 6,9$, which is the value of a for a complete combustion and is near the values used for the correlation. The $CD = 16,737$ CA
- $a = 3$, which is far from the values used for the correlation. The $CD = 14.039$ CA

The start of the combustion is at 717 CA and the shape parameter m is set at 2.085.

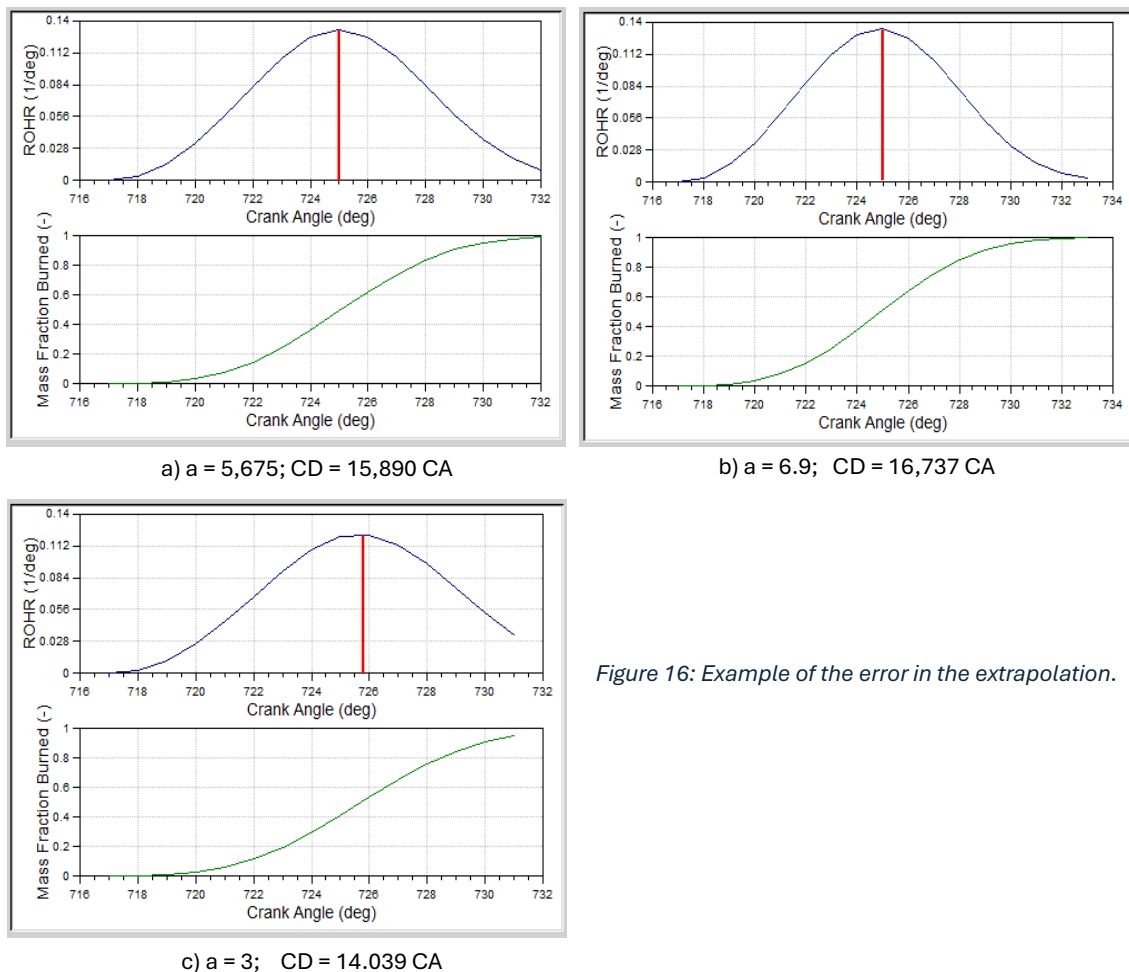


Figure 16: Example of the error in the extrapolation.

6.6. Simulation parameters and approaches

The simulations were conducted with varying parameters to explore their effects on NO_x emissions and engine efficiency. The following approaches are great to show how these engines can be used to carry all types of loads from very low loads until high loads with the possibility of having really low NO_x emissions, with a smaller number of elements. Nonetheless, for each situation every strategy has to be assessed to find the best for the problem presented:

1. **Lambda Variations:** A series of simulations with descending lambda values were performed for both 2000 and 3000 rpm. This approach allows us to understand how lean and rich mixtures affect the combustion process and NO_x formation. By systematically reducing lambda, we aim to identify the optimal air-to-fuel ratio that minimizes NO_x emissions without excessively compromising engine performance.
2. **Compression Ratio (CR) Adjustments:** The compression ratio was varied to observe its impact on NO_x emissions and engine efficiency. Lowering the CR reduces peak combustion temperatures, which can significantly decrease NO_x formation. This series of simulations will help determine the best CR that balances emission reductions with efficient engine operation.
3. **Turbocharger Implementation:** A turbocharger and an intercooler were introduced to improve cylinder filling, aiming to achieve performance competitiveness with gasoline engines. The turbocharger increases the intake air pressure, enhancing the engine's volumetric efficiency and allowing for more fuel to be burned. This leads to higher power output and better overall performance. The impact of different turbocharging pressures on both emissions and performance will be assessed.

Additionally, other potential approaches for NO_x emission reduction were considered but not fully explored in this document. These include the introduction of Exhaust Gas Recirculation (EGR) and exhaust aftertreatment with catalysts to reduce NO_x levels in the exhaust gases [20]. Another approach is water injection, which can cool the combustion chamber, preventing possible abnormal combustion problems, and reduce NO_x formation by lowering peak combustion temperatures [19,27]. Each of these methods has unique advantages and disadvantages, providing a comprehensive understanding of the various strategies available for NO_x reduction.

6.7. Simulation results of the hydrogen engine

This section presents the results of simulations conducted for the hydrogen (H_2) engine using the combustion model defined by the Vibe function with adjusted parameters and the model (The values collected from the results of the simulations, with which these analyses have been carried out, are available in Annex C). The main objective is to evaluate different strategies for reducing NO_x emissions and their impact on engine performance.

6.7.1. Reference values with the Gasoline Model

As a reference for comparison, simulations were conducted using a gasoline engine model example from the program (figure 7), from which the hydrogen engine model was derived. A series of data were obtained for different speed regimes with a stoichiometric mixture of gasoline. Everything else was set by default (Annex A), thus, the compression ratio was $CR = 9$.

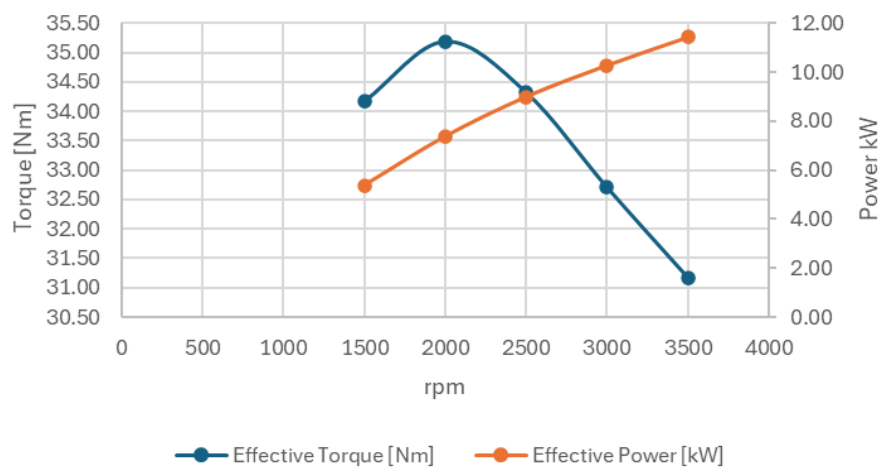


Figure 17: Gasoline performance.

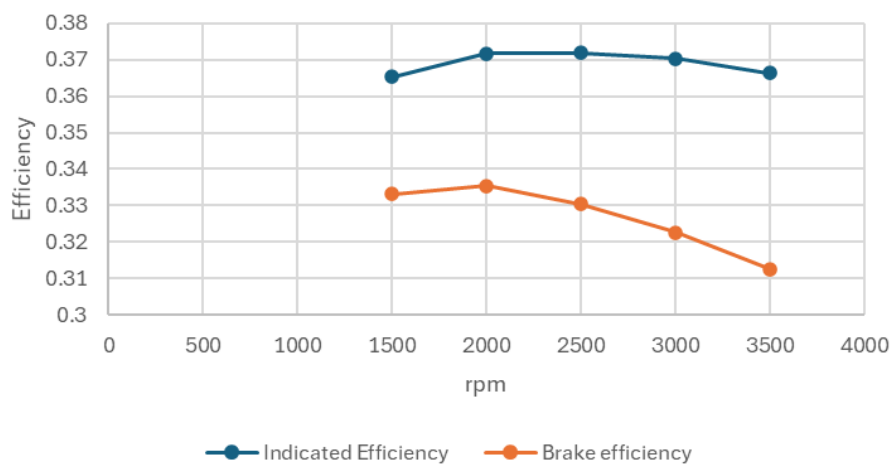


Figure 18: Gasoline efficiency.

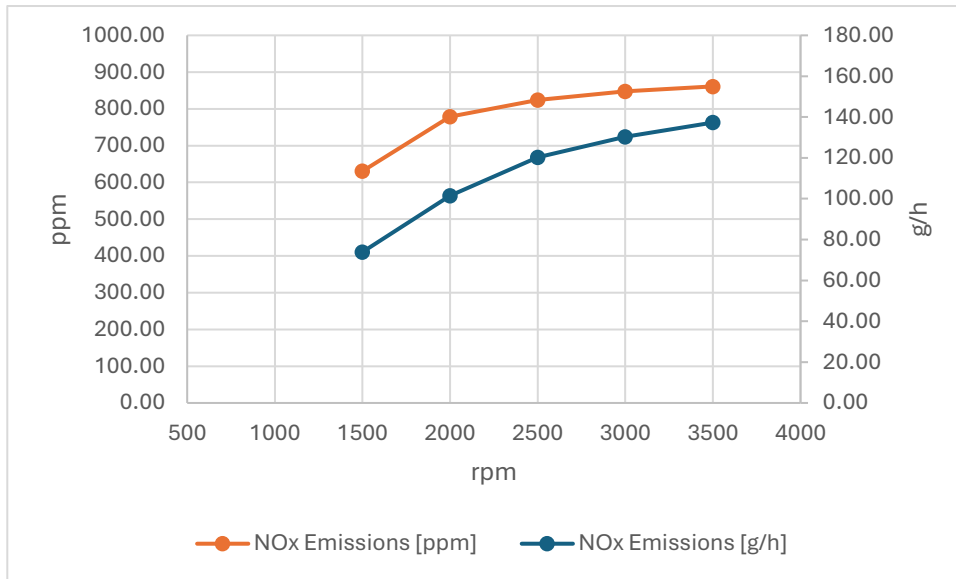


Figure 19: Gasoline NO_x Emissions

The maximum torque provided is at 2000 rpm, being 35.19 Nm and a power of 7.37 kW as seen in table 2. These values will serve as a reference to exceed in terms of performance, always considering NO_x emissions.

Table 2: Gasoline Engine Results

E_Speed [rpm]	Indicated efficiency (-)	Brake efficiency (-)	IMEP [bar]	BMEP [bar]	Effective Torque [Nm]	Effective Power [kW]	NO _x Classic		
							[g/kWh]	[g/h]	[ppm]
1500	0.3654	0.3332	9.4389	8.6089	34.169	5.3672	13.768	73.897	630.487
2000	0.3717	0.3354	9.8262	8.8662	35.190	7.3702	13.763	101.437	778.547
2500	0.3719	0.3303	9.7390	8.6490	34.328	8.9870	13.386	120.298	824.242
3000	0.3703	0.3225	9.4622	8.2422	32.713	10.277	12.683	130.343	847.409
3500	0.3663	0.3126	9.2048	7.8548	31.176	11.427	12.016	137.303	861.109

6.7.2. NO_x Emissions Reduction Strategies

From now on, the simulation results obtained for the hydrogen engine model will be shown. Because the simulations were performed from the information extracted from the fitted ROHR curves of Sementa et al. [17] where the engine CR was equal to 11.5.

6.7.2.1. Lambda Reduction (Lean burn)

The first simulated strategy for reducing NO_x emissions is the reduction of the lambda value. By using lean mixtures, the temperatures inside the cylinder do not exceed 1800°C, a critical threshold for the formation of large amounts of NO_x [19]. The results show a clear trend of decreasing NO_x as the lambda value is reduced. The values used in the graphs are obtained from simulations based on technical paper MTZ 34 1973 (12).

As a consequence of the reduction of hydrogen in the mixture, a significant decrease in engine performance is observed, clearly visible when plotting torque and effective power as a function of lambda in figure 20. However, it is also important to highlight the high efficiency that this type of engine can achieve, as shown in figure 21:

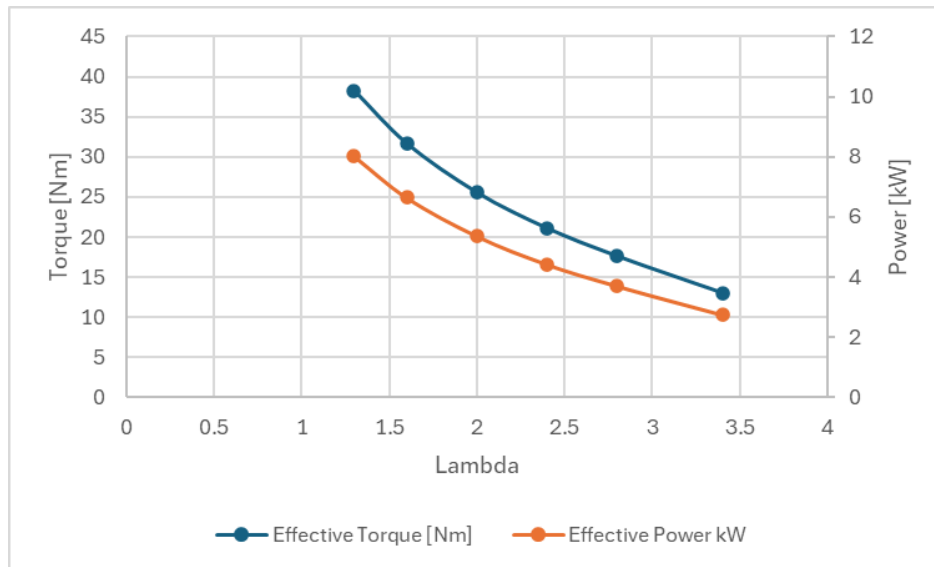


Figure 20: Influence of Lean-burn approach on engine performance.

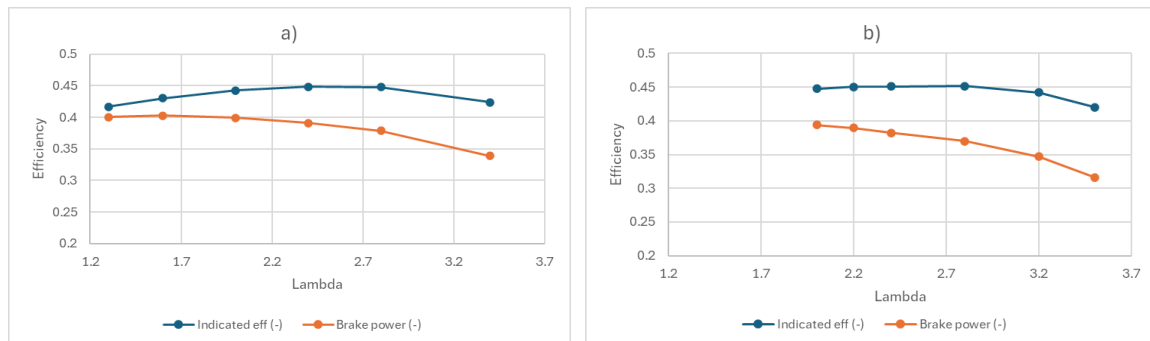


Figure 21: Influence of Lean-burn approach on efficiency for 2000 rpm (a) and 3000 rpm (b) at CR=11.5 cases.

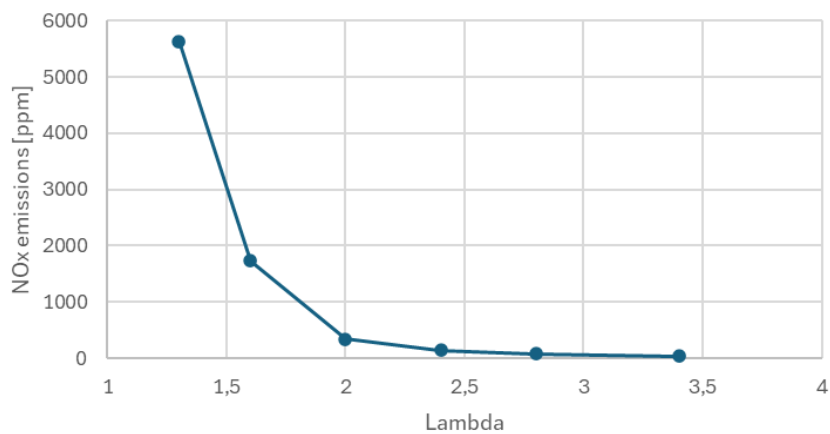


Figure 22: Influence of Lean-burn on NO_x Emissions at 2000 rpm and CR 11.5.

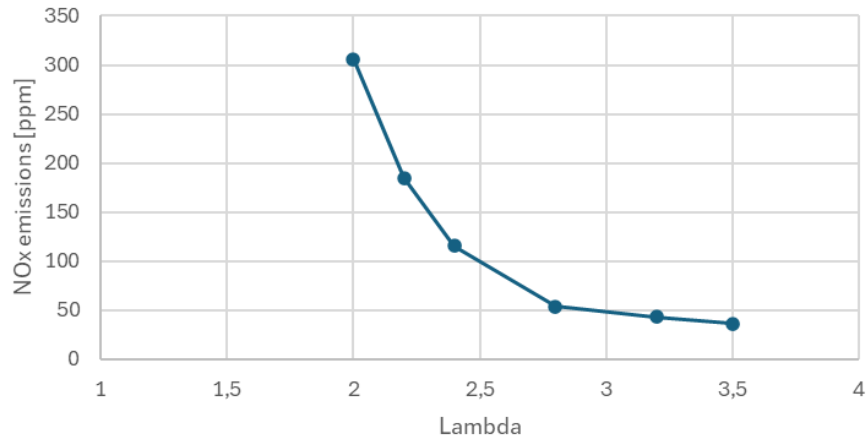


Figure 23: Influence of Lean-burn on NO_x Emissions at 3000 rpm and CR 11.5

6.7.2.2. Compression Ratio Reduction (CRR)

Another strategy to reduce NO_x emissions in the hydrogen engine is the reduction of the compression ratio. By reducing the CR, the mixture begins combustion at lower pressure and temperature, which decreases the temperature reached during combustion and, therefore, NO_x emissions, as can be seen in the following figure 24. Although changing the CR would alter hydrogen combustion, the parameters of the Vibe function were kept unchanged for simplicity. These simulations were conducted for $\lambda = 2$, a point where emissions show a change in trend while maintaining good efficiency.

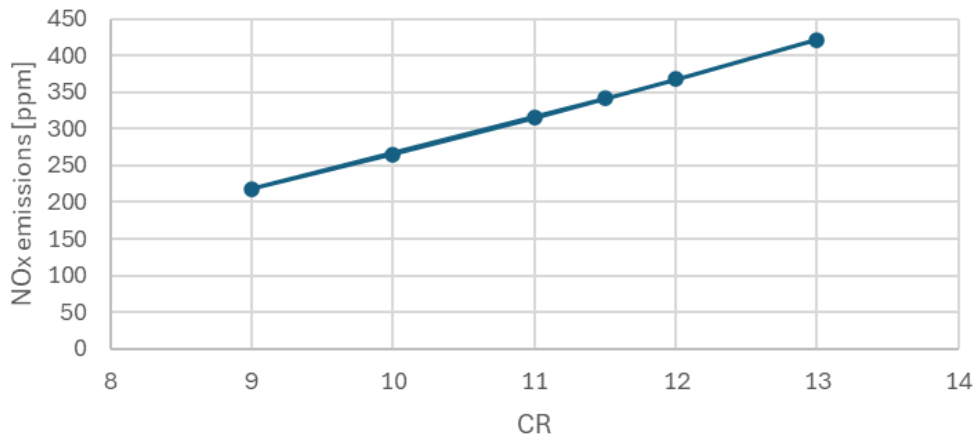


Figure 24: Influence of the change of CR on NO_x Emissions at 2000 rpm and lambda = 2

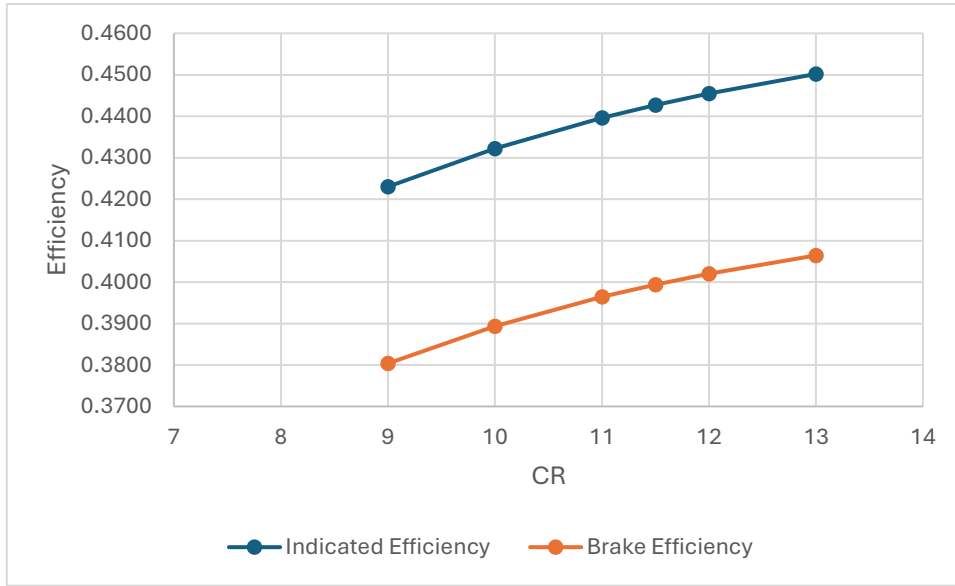


Figure 25: Influence of the change of CR on the efficiency at 2000 rpm and $\lambda = 2$

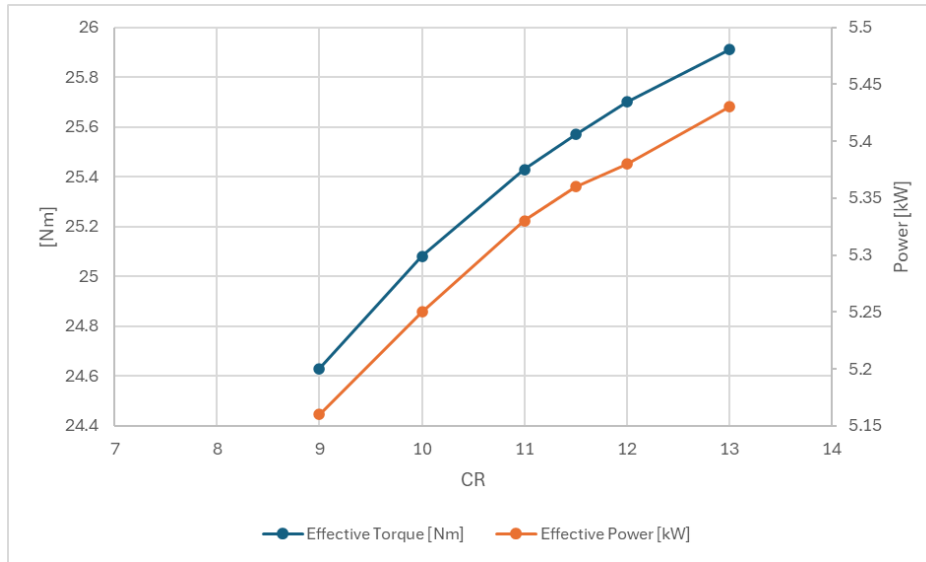


Figure 26: Influence of the change of CR on the performance at 2000 rpm and $\lambda = 2$

6.7.3. Influence of emission reduction strategies on performance

Changing the compression ratio does not significantly affect performance or emissions as much as reducing λ , this tendency is appreciable in figure 27. However, reducing λ can notably influence efficiency. The table 3 compares the two strategies, demonstrating that emission reductions strategies are often followed by a decrease in engine performance.

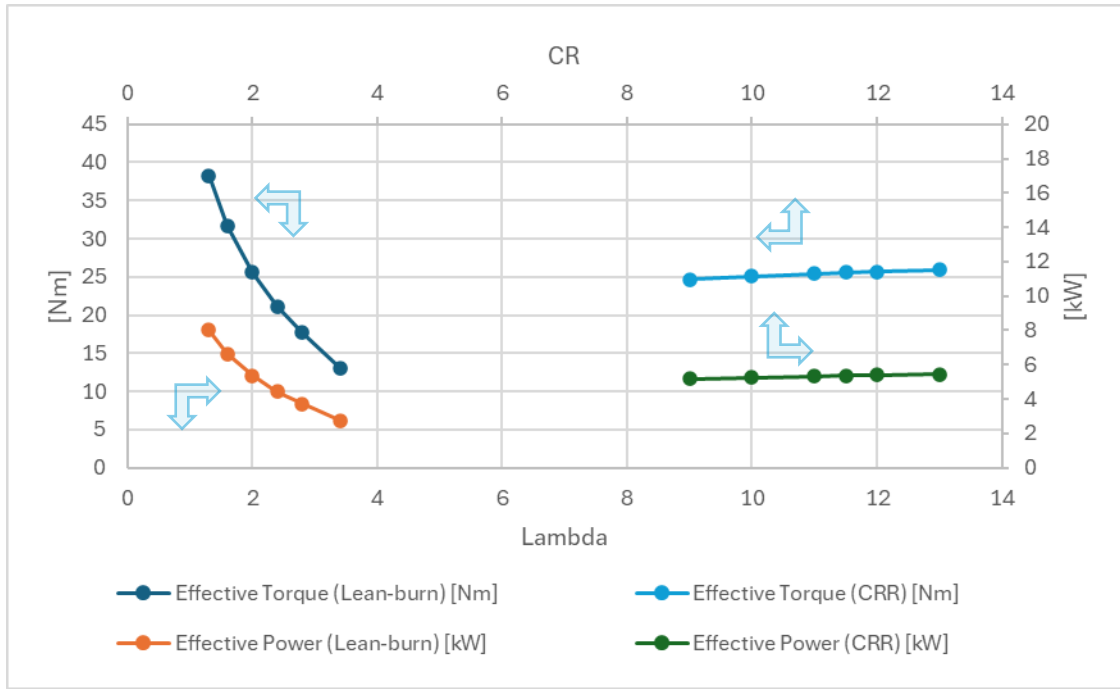


Figure 27: Comparison of the influence of both approaches of reduction emission on the performance.

Table 3: Main results of the simulations. Firstly, the results of the lean-burn approach are shown, and secondly, the results of CR reduction are shown.

E_Speed	CR	Lambda	Indicated efficiency	Brake efficiency	IMEP	BMEP	Effective Torque	Effective Power		NO _x Classic	
[rpm]	(-)	(-)	(-)	(-)	[bar]	[bar]	[Nm]	[kW]	[PS]	[g/h]	[ppm]
2000	11.5	1.3	0.4166	0.4005	10.652	9.643	38.27	8.02	10.9	189.881	5635.65
2000	11.5	1.6	0.4304	0.4027	8.991	7.982	31.68	6.64	9.02	56.669	1736.32
2000	11.5	2	0.4427	0.3994	7.454	6.444	25.57	5.36	7.28	10.849	341.66
2000	11.5	2.4	0.4483	0.3913	6.335	5.323	21.13	4.42	6.02	4.230	135.68
2000	11.5	2.8	0.4476	0.3790	5.461	4.448	17.65	3.7	5.03	2.432	79.01
2000	11.5	3.4	0.4236	0.3386	4.305	3.291	13.06	2.74	3.72	1.125	37.02
3000	11.5	2	0.4478	0.3937	7.705	6.397	25.39	7.98	10.85	14.722	305.87
3000	11.5	2.2	0.4503	0.3892	7.076	5.768	22.89	7.19	9.78	8.822	185.17
3000	11.5	2.4	0.4509	0.3822	6.525	5.217	20.71	6.5	8.84	5.463	115.65
3000	11.5	2.8	0.4515	0.3697	5.648	4.341	17.23	5.41	7.36	2.508	53.84
3000	11.5	3.2	0.4419	0.3470	4.884	3.577	14.2	4.46	6.06	1.979	42.94
3000	11.5	3.5	0.4204	0.3160	4.289	2.983	11.84	3.72	5.06	1.667	36.37
2000	9	2	0.4230	0.3804	7.454	6.444	24.63	5.16	7.01	6.972	217.88
2000	10	2	0.4322	0.3893	7.214	6.205	25.08	5.25	7.14	8.466	265.5
2000	11.5	2	0.4427	0.3994	7.329	6.319	25.57	5.36	7.28	10.849	341.66
2000	11	2	0.4396	0.3964	7.418	6.407	25.43	5.33	7.24	10.039	315.73
2000	12	2	0.4455	0.4020	7.486	6.476	25.7	5.38	7.32	11.673	368.06
2000	13	2	0.4502	0.4064	7.539	6.528	25.91	5.43	7.38	13.355	421.98

6.7.4. Turbocharger implementation

Due to the reduction in engine performance with the implementation of NO_x emission reduction strategies, it was decided to introduce a turbocharger with an intercooler (TCI). Therefore, as shown in the figure 28, the model was modified to include a turbocharger and an intercooler in the cylinder intake. It was adjusted based on the turbocharger from the example program `tcimcmz_3cyl` and the program documentation. This decision was made to increase the engine's volumetric and thermal efficiency, thus allowing more fuel to be introduced while maintaining the same air/fuel ratio, improving effective mean pressures, and enhancing engine performance.

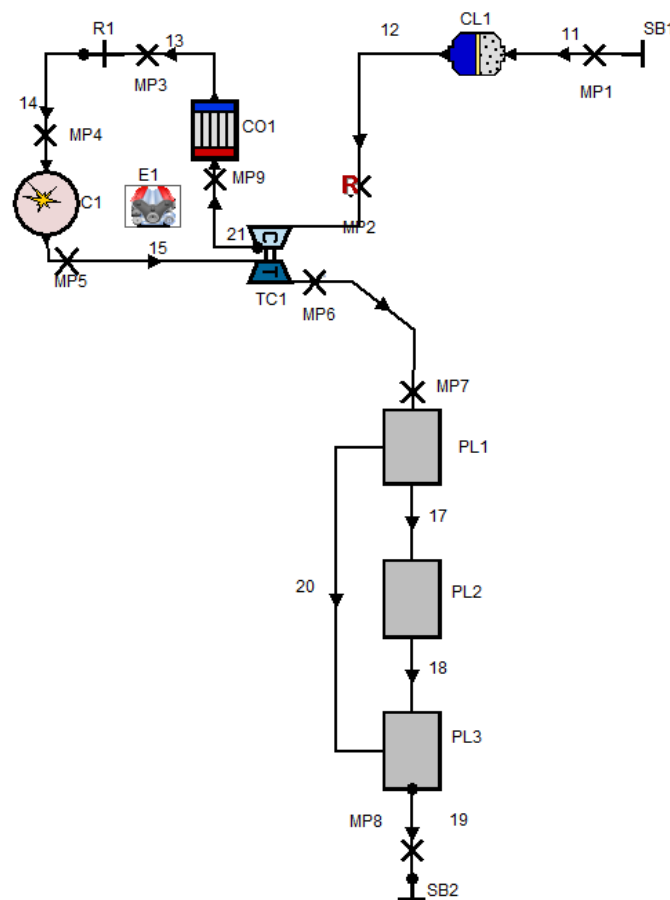


Figure 28: Modification of the model to include a Turbocharged and intercooler.

A challenge in implementing a turbo in a single-cylinder engine is the irregularity of the flow in the compressor, as it only has one exhaust gas discharge to the turbine. Additionally, as shown in figure 29, the compressor flow with a low-pressure ratio can reach zero, which is undesirable. Nevertheless, this approach helps understand emission trends and performance improvements, which are applicable to engines with more cylinders.

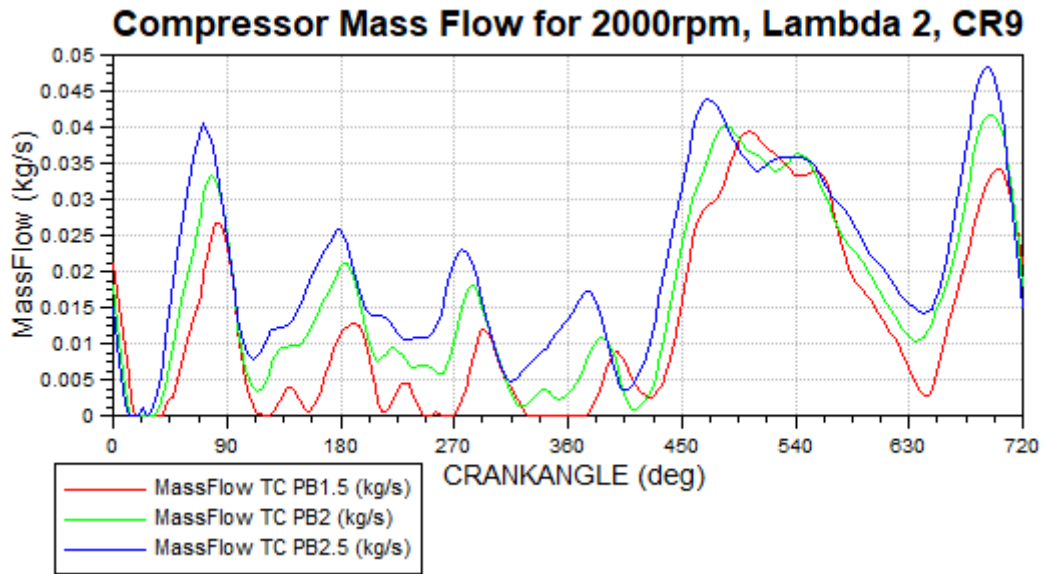


Figure 29: Compressor Mass Flow for different Pressure Boost (PB) at 2000rpm, Lambda = 2 and CR = 9 from simulations applying compression ratio reduction (Section 6.7.5.1)

Tests were conducted with Lambda = 2 and CR = 11.5 to analyse the influence of the turbocharger at different "pressure boost" levels in the compressor (1.5, 2, and 2.5 bar). However, because of the efficiency it would be less. The figure 30 shows how this strategy influences emissions in comparison with the case without the TCI system the emission grows with the pressure boost, and it tends to grow potentially.

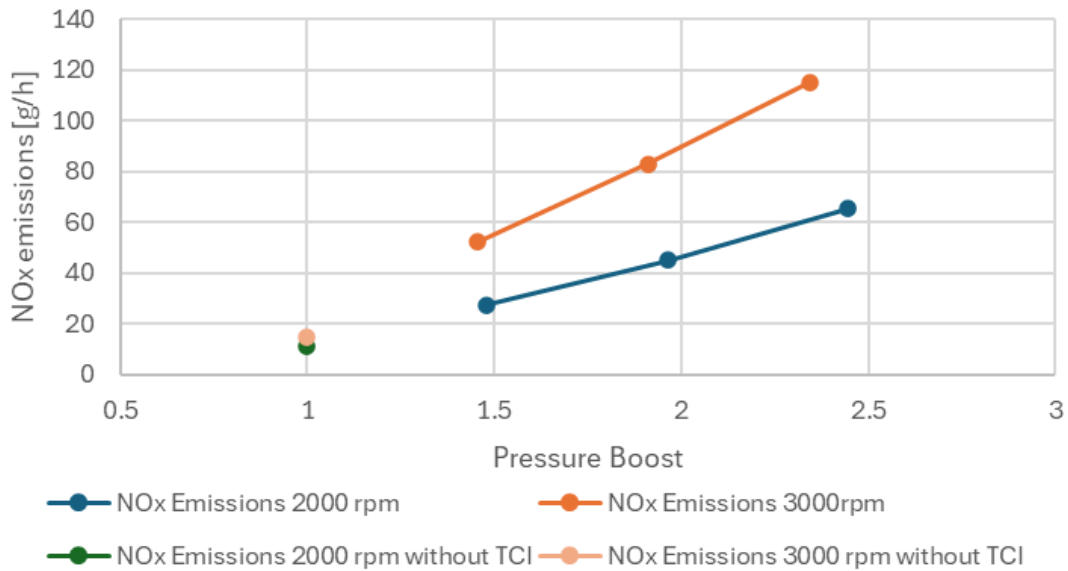


Figure 30: Influence of the TCI system in the NO_x emissions.

The graphics in figure 31 show how as more pressure boost is delivered more efficiency is obtain, this is higher in the 2000 rpm case than in the 3000 rpm. However, it tends to slow to reach a maximum around 2.8 bar in both cases.

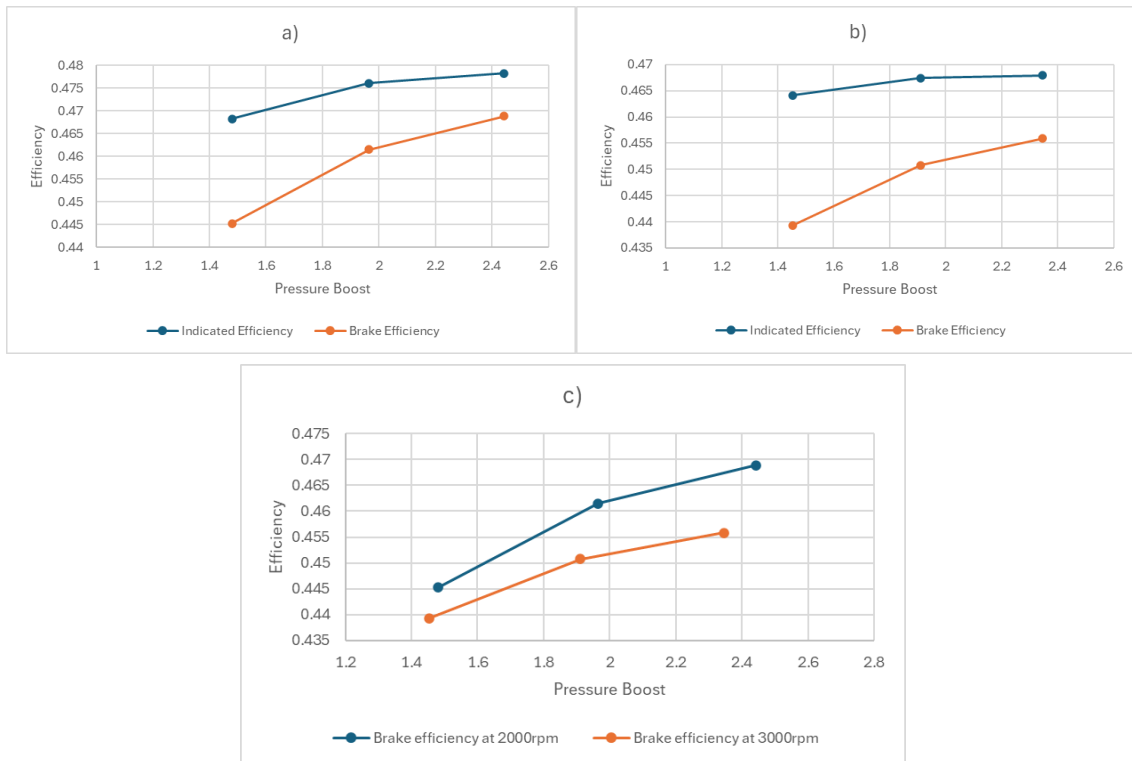


Figure 31: influence of Turbocharger on the efficiency for $\lambda = 2$ and $CR = 11.5$; a) efficiency at 2000 rpm; b) efficiency at 3000 rpm; c) comparison of efficiencies

Bellow, in table 4 is shown the overall performance for the cases simulated with the TCI model and is compared with the case that do not have it. It can be seen in figure 32 that as the pressure boost rise the mean effective pressure rise and, thus, the effective power and torque increased. The reached BMEP values with this pressure boost values are higher than the gasoline fuelled engine. Even though the NO_x emissions are high and rises with higher pressure boost values, they are still lower than the gasoline engine's NO_x emissions.

Table 4: Global performance comparison between H2 ICE at 2000 rpm, $\lambda = 2$ and $CR = 11.5$ with and without TCI for different pressure boost

Pressure Boost [bar]	IMEP [bar]	BMEP [bar]	Effective Torque [Nm]	Effective Power		NO_x Emissions [ppm]
				[kW]	[PS]	
0	7.454	6.444	25.57	5.36	7.28	341.66
1.4805	11.994	11.407	45.27	9.48	12.89	531.66
1.9651	15.879	15.556	61.74	12.93	17.58	656.58
2.4429	19.659	19.486	77.34	16.2	22.02	773.5

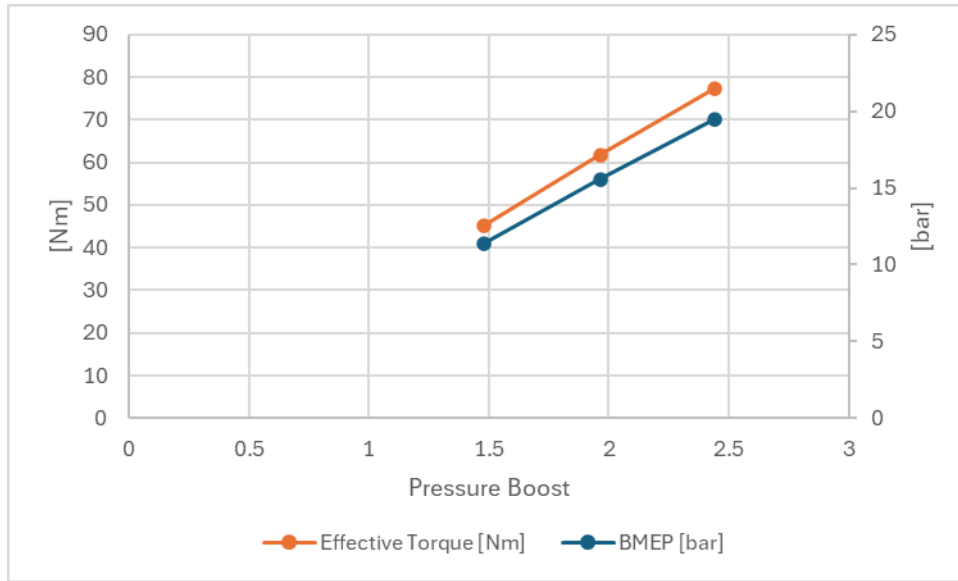


Figure 32: Influence of the Pressure Boost in the BEMP and Torque at 2000 rpm, Lambda = 2 and CR = 11.5

6.7.5. Testing of reduction strategies with turbocharger

After achieving an increase in effective mean pressure to values higher than those of the gasoline engine and due to the increase in emissions, the previously tested strategies were re-applied separately.

6.7.5.1. Compression Ratio Reduction

The compression ratio reduction strategy was applied to evaluate its behaviour with the turbocharger. The value choose was CR = 9 to match the value of the gasoline model. In the table 5, it can be seen how, **emissions improve without a significant worsening of performance** compering with the previous case shown in the table 4. Which has with the same Lambda = 2, but with CR = 11.5,

Table 5: Global performance comparison between H2 ICE at 2000 rpm, Lambda = 2 and CR = 9 with and without TCI for different pressure boost.

Pressure Boost [bar]	IMEP [bar]	BMEP [bar]	Effective Torque [Nm]	Effective Power		NO _x Emissions [ppm]
				[kW]	[PS]	
0	7.454	6.444	25.57	5.36	7.28	341.66
1.4801	11.683	11.104	44.07	9.23	12.55	356.69
1.9643	15.459	15.196	60.31	12.63	17.17	446.76
2.4414	19.128	19.076	75.71	15.86	21.56	532.46

Following, in figure 34 it can be observed how the efficiency decay for both reduction emissions strategies in comparison with the TCI H2 model. However, efficiency lean-burn approach does not decay more than 1% per 0.8 decrease of lambda. This is remarkably, because as will be seen bellow the lean-burn approach obtain less NO_x emissions than the CRR approach. Nevertheless, lean-burn detriment BMEP more than CRR approach.

6.7.5.2. *Lambda Reduction (Lean-burn)*

The lambda reduction strategy was applied, achieving better results as burning with lean mixtures achieves similar mean effective mean pressures and performance to those of the gasoline engine, while also achieving lower emission values. The exception that is below the gasoline engine values is the case of pressure ratio = 1.5 at 2000 rpm (Pressure Boost = 1.4801).

Table 6: Global performance comparison between H2 ICE at 2000 rpm, Lambda = 2.8 and CR = 11.5 with and without TCI for different pressure boost.

Pressure Boost [bar]	IMEP [bar]	BMEP [bar]	Effective Torque [Nm]	Effective Power		NO _x Emissions [ppm]
				[kW]	[PS]	
0	7.454	6.444	25.57	5.36	7.28	341.66
1.4801	8.754	8.083	32.08	6.72	9.13	118.69
1.9643	11.588	11.017	43.73	9.16	12.45	145.16
2.4414	14.549	14.017	55.63	11.65	15.84	165.35

Table 7: Global performance comparison between H2 ICE at 3000 rpm, Lambda = 2.8 and CR = 11.5 with and without TCI for different pressure boost.

Pressure Boost [bar]	IMEP [bar]	BMEP [bar]	Effective Torque [Nm]	Effective Power		NO _x Emissions [ppm]
				[kW]	[PS]	
0	7.454	6.444	25.57	5.36	7.28	341.66
1.4801	10.5423	9.2626	36.76	11.55	15.7	104.4
1.9643	13.8746	12.4739	49.51	15.55	21.15	124.22
2.4414	17.2908	15.6918	62.28	19.57	26.6	135.05

Usually, the NO_x emissions in both ppm and g/h units show the same trend. But with the introduction of turbocharger the tendency does not always goes in the same way. Figure 33 shows the trend of NO_x emissions for different boost pressures and engine revolutions. The NO_x emissions in ppm at 3000 rpm (choppy line) may suggest that the NO_x emissions start to slow, but if we look at NO_x emissions in g/h at 3000 rpm it keeps a grow trend because of the higher engine speed. Therefore, for the analysis of NO_x emissions, the engine speed and how the NO_x emissions will accumulate through time due to the engine speed must also be considered.

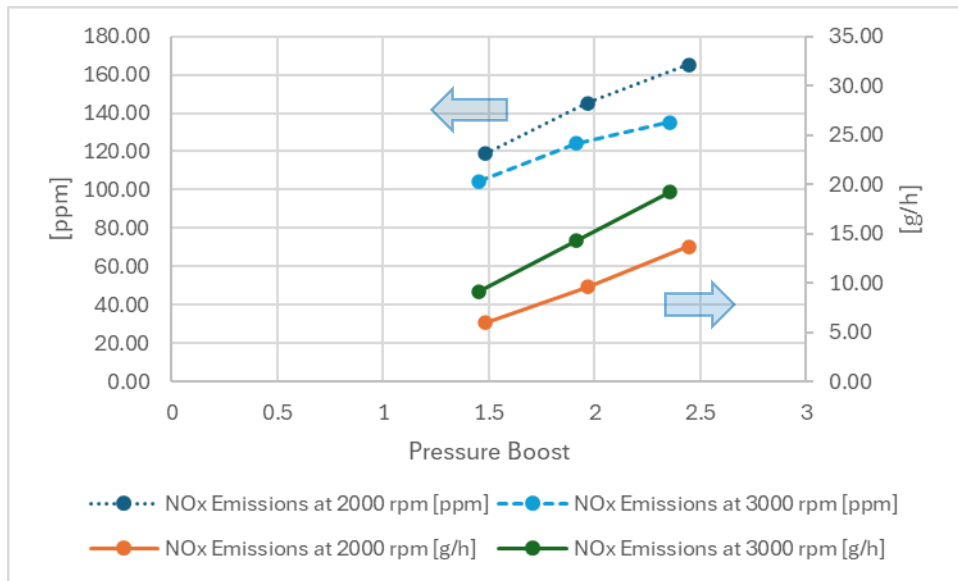


Figure 33: Consideration of engine speed in the analysis of the NO_x emissions after the introduction of the TCI system, data obtain at Lambda = 2.8 and CR = 11.5.

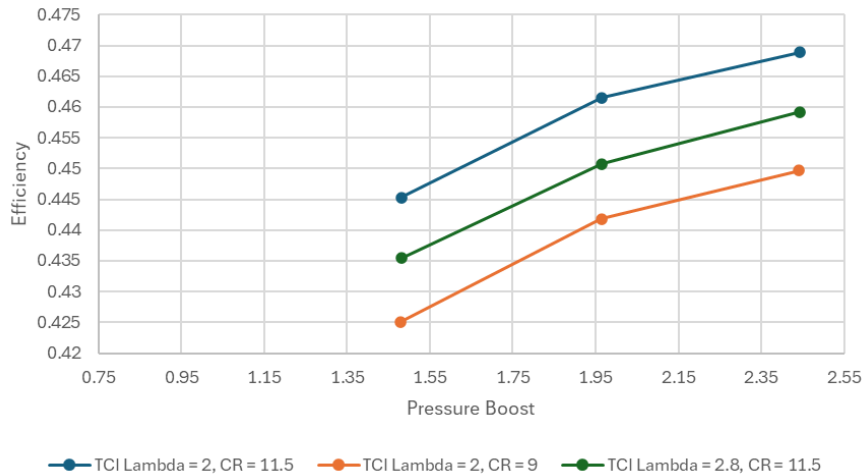


Figure 34: Brake efficiency comparison at 2000 rpm between the different cases studied after the introduction of the TCI system. Blue for baseline, orange for CR reduction and green for Lean-burn approach.

6.7.6. Combination of strategies

Finally, it was decided to combine both strategies: compression ratio reduction and lambda reduction, along with the implementation of the turbocharger. This combination showed a significant improvement in engine performance without a major detriment to emissions, as shown in the following figure 36 and tables 8 and 9.

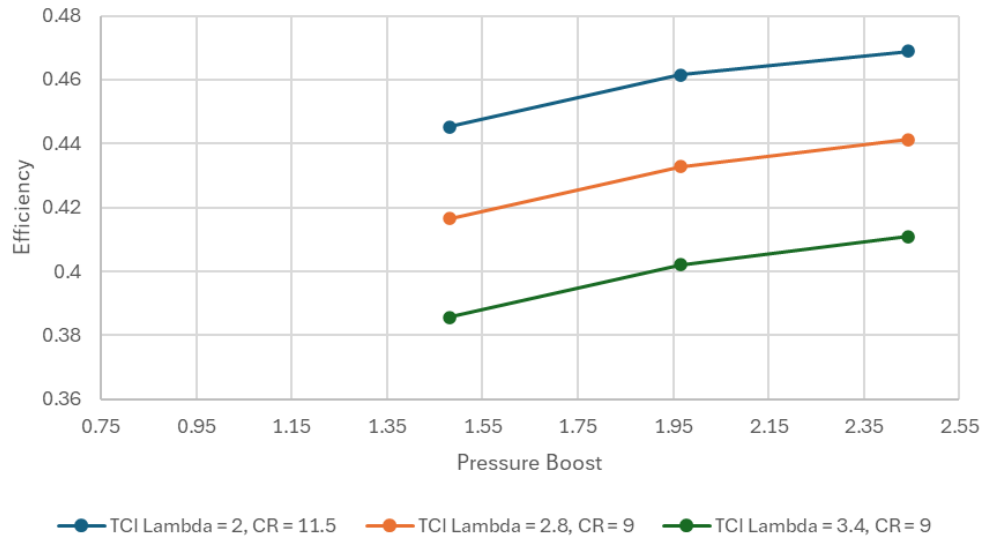


Figure 35: Brake efficiency comparison at 2000 rpm between the reference in the TCI (blue) and the combination approaches for two different lambdas.

Bellow, table 8 and table 9 show the two set of simulations evaluated for the combination of strategies. In the first table (table 8) is possible to see different performance parameters. From which the vast majority are similar to the ones obtain by the gasoline engine, except the results for engine speed 2000 rpm with Pressure Boost = 1.4802 bar.

Table 8: Summary of the simulations with the combination of the approaches with CR = 9 and Lambda taking values of 2.8, 3.4 and 3.5

E_Speed	CR	Lambda	Pressure Boost	Indicated efficiency	Brake efficiency	IMEP	BMEP	Effective Torque	Effective Power	
[rpm]	(-)	(-)	[bar]	(-)	(-)	[bar]	[bar]	[Nm]	[kW]	PS
2000	9	2.8	1.4802	0.4570	0.4166	8.538	7.901	31.36	6.57	8.93
2000	9	2.8	1.9646	0.4622	0.4327	11.306	10.822	42.95	9	12.23
2000	9	2.8	2.4428	0.4643	0.4413	14.223	13.818	54.84	11.49	15.62
3000	9	2.8	1.4532	0.4444	0.4035	10.210	8.956	35.55	11.17	15.18
3000	9	2.8	1.9093	0.4455	0.4155	13.430	12.075	47.92	15.06	20.47
3000	9	2.8	2.3501	0.4453	0.4224	16.735	15.185	60.27	18.93	25.74
2000	9	3.4	1.4802	0.4370	0.3857	6.723	6.047	24	5.03	6.83
2000	9	3.4	1.9647	0.4401	0.4021	8.888	8.305	32.96	6.9	9.39
2000	9	3.4	2.4431	0.4411	0.4110	11.167	10.618	42.14	8.83	12
3000	9	3.5	1.4533	0.4156	0.3619	7.771	6.464	25.66	8.06	10.96
3000	9	3.5	1.9096	0.4154	0.3751	10.211	8.766	34.79	10.93	14.86
3000	9	3.5	2.3504	0.4143	0.3827	12.724	11.068	43.93	13.8	18.76

In concern of the NO_x emissions, the simulations allow to believe that it is possible to obtain values near zero in comparison to the gasoline engine with aftertreatment. Moreover, these combinations allow to have really low emissions, but with a competitive performance.

Table 9: Summary of NO_x emissions for the set simulation of combination of approaches.

E_Speed [rpm]	CR (-)	Lambda (-)	Pressure Boost [bar]	NO _x Classic	
				[g/h]	[ppm]
2000	9	2.8	1.4802	3.518	69.12
2000	9	2.8	1.9646	5.807	86.08
2000	9	2.8	2.4428	8.363	99.02
3000	9	2.8	1.4532	5.237	59.01
3000	9	2.8	1.9093	8.241	70.72
3000	9	2.8	2.3501	10.949	75.80
2000	9	3.4	1.4802	1.568	31.25
2000	9	3.4	1.9647	2.569	38.66
2000	9	3.4	2.4431	3.664	44.11
3000	9	3.5	1.4533	3.328	38.08
3000	9	3.5	1.9096	5.201	45.40
3000	9	3.5	2.3504	6.959	49.08

7. Conclusions

When hydrogen is generated without emissions through the use of renewable energies (green hydrogen), and because as a fuel, it does not emit greenhouse gases and most of the pollutants that a conventional fuel generates during the combustion process; it can be considered as one of the best fuels for sustainable mobility, as it only generates water vapour and nitrogen oxides, which can be eliminated in several ways. Some of these have been successfully demonstrated in this study.

The reduction of lambda and the compression ratio are effective strategies to decrease NO_x emissions in a hydrogen engine, but at the expense of reducing engine performance. The implementation of a turbocharger improves performance but increases emissions. Nevertheless, the combination of these strategies with the turbocharger allows a balance between emission reduction and maintaining acceptable performance. However, the level of implementation of these strategies will depend on the situation faced, the load the engine must withstand and the maximum NO_x emissions available. It is possible that if such low emission levels as in table 8 are not needed, you can dispense with lowering the CR. Even if it is needed to cope with high loads, it could use higher CR and/or increase the boost pressure delivered by the turbocharger.

The simulation results can be considered satisfactory considering the trends they show. However, they cannot be taken as absolute values because, although vbe function is widely used in combustion simulation and can get satisfactory results. It can be too ideal. Besides the simulations were set to make the complete combustion, thus, there is the possibility that both NO_x emissions and performance were lower.

Unfortunately, the current production of hydrogen is mostly concentrated in generating grey hydrogen, while green hydrogen is less than 1%. It is important to start changing this state for the following years if the proliferation of H₂ICE is wanted. Because it can happen the same as other ecofriendly mobility sectors like BEV or HEV. Where companies are making cars that get zero emissions, but then, the costs to obtain the fuel or materials needed for the car pollutes more or does more harm to the environment, than the benefits provided by the car.

On the positive side, recent advancements in hydrogen combustion and storage research have been significant. A main challenge for the large-scale introduction of hydrogen in low-duty vehicles is addressing hydrogen storage and direct injection technologies. Given current constraints related to space availability, battery life, and

recharging, heavy-duty vehicles present a promising opportunity for the application of hydrogen technology. These vehicles can utilize hydrogen not only in traditional engines but also in conjunction with hybrid technology.

REFERENCIAS

- [1] Al-Baghdadi, M. A. S. (2004). Effect of compression ratio, equivalence ratio and engine speed on the performance and emission characteristics of a spark ignition engine using hydrogen as a fuel. *Renewable Energy*, 29(15), 2245-2260.
<https://doi.org/10.1016/j.renene.2004.04.002>
- [2] A comprehensive and science-based terminology, classification and taxonomy for hydrogen. Draft for discussion| UNECE. (2022, 26 septembre).
https://unece.org/sites/default/files/2022-08/ECE_ENERGY_2022_8e.pdf
- [3] *Alternative fuels* | *European Alternative Fuels Observatory*. (s. f.).
<https://alternative-fuels-observatory.ec.europa.eu/general-information/alternative-fuels>
- [4] Andrea W. (28th of July of 2022) The colors of hydrogen: Expanding ways of decarbonization. (s. f.). *Spectra*. <https://spectra.mhi.com/the-colors-of-hydrogen-expanding-ways-of-decarbonization>
- [5] Corporativa, I. (s. f.). *Diferencia entre hidrógeno verde y azul - Iberdrola*. Iberdrola.
<https://www.iberdrola.com/conocenos/nuestra-actividad/hidrogeno-verde/diferencia-hidrogeno-verde-azul>
- [6] Das, L. M. (2007). The potential of hydrogen as an alternative fuel for the transport and power sector in India. *International Journal of Environmental Studies*, 64(6), 749–759. <https://doi.org/10.1080/00207230701770418>
- [7] Das, L. (2016). Hydrogen-fueled internal combustion engines. In *Elsevier eBooks* (pp. 177-217). <https://doi.org/10.1016/b978-1-78242-363-8.00007-4>
- [8] *Euro 7: New proposal for vehicle emissions type approval in Europe. Presentation at GRPE 87*. (2023, January 12). UNECE Retrieved April 22, 2024, from <https://unece.org/sites/default/files/2023-01/GRPE-87-37r1e.pdf>
- [9] *Euro 7: Parliament adopts measures to reduce road transport emissions* | *News* | *European Parliament*. (n.d.). <https://www.europarl.europa.eu/news/en/press-room/20240308IPR19017/euro-7-parliament-adopts-measures-to-reduce-road-transport-emissions>
- [10] Fernández-Bolaños, C. (2005) 3.2 Almacenamiento del hidrógeno. *Energética del hidrógeno: contexto, estado actual y perspectiva de future*, p127-149.
<https://biblus.us.es/bibing/proyectos/abreproy/3823/fichero/3.2+Almacenamiento+del+Hidr%C3%B3geno.pdf>
- [11] Gamez, M. J. (2022, May 24). *Objetivos y metas de desarrollo sostenible - Desarrollo Sostenible*. Desarrollo Sostenible.
<https://www.un.org/sustainabledevelopment/es/objetivos-de-desarrollo-sostenible/>
- [12] Genia. (2023, May 5). *Los diferentes tipos de hidrógeno según sus colores*. Genia Global Energy. <https://geniaglobal.com/tipos-de-hidrogeno-segun-colores/>
- [13] González, P. G. (2022, March 18). *Los colores del hidrógeno: verde, gris, azul y rosa o magenta*. Restauración De Ecosistemas.
<https://www.restauraciondeecosistemas.com/los-colores-del-hidrogeno-verde-gris-azul-rosa-magenta/>
- [14] *Hidrógeno - Centro Nacional del Hidrógeno*. (2019, February 6). Centro Nacional del Hidrógeno. <https://www.cnh2.es/el-hidrogeno/#tab-id-1>

- [15] Hydrogen storage. (n.d.). Energy.gov. <https://www.energy.gov/eere/fuelcells/hydrogen-storage#:~:text=Storage%20of%20hydrogen%20as%20a,pressure%20is%20%E2%88%92252.8%C2%B0C>.
- [16] Martin. (2023, October 19). *Energy - United Nations Sustainable Development*. United Nations Sustainable Development. <https://www.un.org/sustainabledevelopment/energy/>
- [17] Sementa, P., De Vargas Antolini, J. B., Tornatore, C., Catapano, F., Vaglieco, B. M., & Sánchez, J. J. L. (2022). Exploring the potentials of lean-burn hydrogen SI engine compared to methane operation. *International Journal of Hydrogen Energy*, 47(59), 25044–25056. <https://doi.org/10.1016/j.ijhydene.2022.05.250>
- [18] *Sitio web del Hidrógeno*. (s. f.). Ministerio Para la Transición Ecológica y el Reto Demográfico. <https://www.miteco.gob.es/es/energia/hidrocarburos-nuevos-combustibles/hidrogeno.html>
- [19] Stępień, Z. (2021). A Comprehensive Overview of Hydrogen-Fueled Internal Combustion Engines: Achievements and Future Challenges. *Energies*, 14(20), 6504. <https://doi.org/10.3390/en14206504>
- [20] Sterlepper, S., Fischer, M., Claßen, J., Huth, V., & Pischinger, S. (2021). Concepts for Hydrogen Internal Combustion Engines and Their Implications on the Exhaust Gas Aftertreatment System. *Energies*, 14(23), 8166. <https://doi.org/10.3390/en14238166>
- [21] The many colours of hydrogen | Sustainable NI. (s. f.). <https://www.sustainableni.org/blog/many-colours-hydrogen>
- [22] UNECE to develop international hydrogen classification system | UNECE. (2022, 26 septiembre). <https://unece.org/climate-change/press/unece-develop-international-hydrogen-classification-system>
- [23] United Nation. Infographic: Climate Change. https://www.un.org/sustainabledevelopment/wp-content/uploads/2023/08/2309739_E_SDG_2023_infographics-13-13.pdf
- [24] Verhelst, S. (2014). Recent progress in the use of hydrogen as a fuel for internal combustion engines. *International Journal Of Hydrogen Energy*, 39(2), 1071-1085. <https://doi.org/10.1016/j.ijhydene.2013.10.102>
- [25] Verhelst, S., Demuyneck, J., Sierens, R., Scarcelli, R., Matthias, N. S., & Wallner, T. (2013). Update on the Progress of Hydrogen-Fueled Internal Combustion Engines. *En Elsevier eBooks* (pp. 381-400). <https://doi.org/10.1016/b978-0-444-56352-1.00016-7>
- [26] Verhelst, S., & Sierens, R. (2007). A quasi-dimensional model for the power cycle of a hydrogen-fuelled ICE. *International Journal of Hydrogen Energy*, 32(15), 3545–3554. <https://doi.org/10.1016/j.ijhydene.2007.02.011>
- [27] Verhelst, S., & Wallner, T. (2009). Hydrogen-fueled internal combustion engines. *Progress In Energy And Combustion Science*, 35(6), 490-527. <https://doi.org/10.1016/j.pecs.2009.08.001>
- [28] Wang, L., Li, X., Hong, C., Guo, P., Guo, S., & Yang, Z. (2023). Research and Development of Hydrogen-Fueled Internal Combustion Engines in China. *ACS Omega*, 8(51), 48590-48612. <https://doi.org/10.1021/acsomega.3c05397>

ANNEX A: Boundary condition and initialization set up.

All simulations are configured with these elements in common.

Starting with simulation control:

The image shows a software interface for 'Cycle Simulation' with the following settings:

- Species Transport: General
- Non-Engine Application:
 - Reference Speed: [] rpm
 - Reference Cycle Type: 4-Stroke, 2-Stroke, Rotary Piston Engine
- Simulation Interval:
 - End of Simulation: 30 cycle(s)
 - Convergence Control
- Spatial Pipe Discretization:
 - Average Cell Size: 25 mm
 - Simulation Step Size: [] deg
 - CFL Multiplier: []

Figure 36: Simulation Control: Cycle Simulation

In the Engine element, the firing order is set in 0 degrees of Crack angle, and it was kept as so for every simulation. Also with the friction model, it was kept by default.

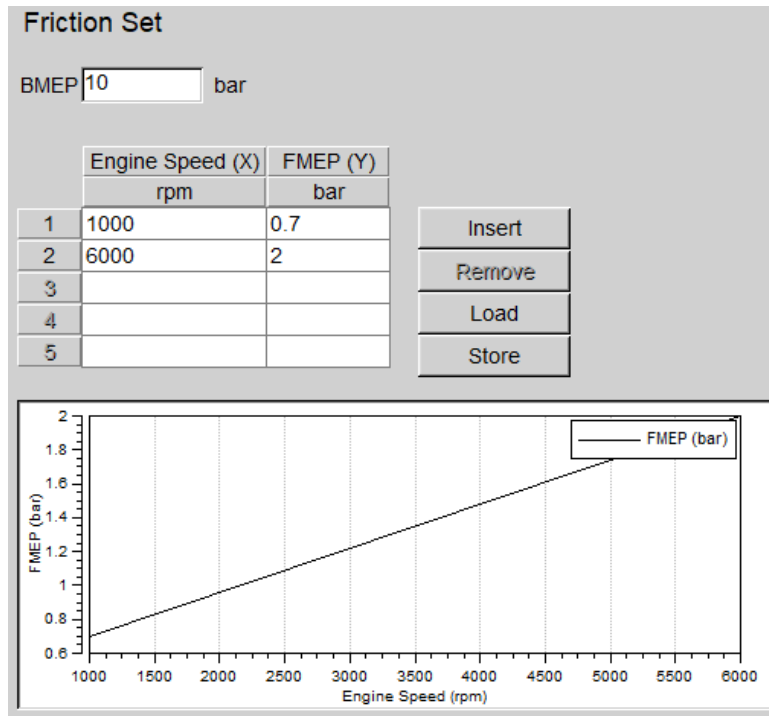


Figure 37: Engine: Friction set.

Air Cleaner it was kept as default:

General

Author

Comment

Result Name Date

Geometrical Properties

Total Air Cleaner Volume l

Inlet Collector Volume l

Outlet Collector Volume l

Length of Filter Element mm

Hydraulic Setting of Filter Element

Hydraulic Setting

Hydraulic Unit Diameter Area

Hydraulic Diameter mm

Hydraulic Area mm²

Figure 38: Air Cleaner: General

All the flow coefficients are set at 0.95.

For Cylinder element:

General

Author

Comment

Result Name Date

Bore mm

Stroke mm

Compression Ratio [-]

Con-Rod Length mm

Piston Pin Offset mm

Effective Blow By Gap mm

Mean Crankcase Press. bar

User Defined Piston Motion

Chamber Attachment

Scavenge Model

Figure 39: Cylinder: General (Geometry).

Each Plenum is 1.8 Liters. Their flow coefficients have the value of 0.98 except in plenum 3 where the flow coefficients related to 11 takes the value of 0.5. Finally, the initialisation uses the set 1 from simulation control.

For **Gasoline Simulation** everything is keep as default.

Default set up simulation control (Gasoline):

General Species Setup

Species Set

	Species
1	GASOLINE
2	O2
3	N2
4	CO2
5	H2O

Homogenous Reaction Set

	Key	Chemistry
1		
2		
3		
4		
5		

Fuel Species Set

Mass Based Fractions Volume Based Fractions

	Fuel Species	Mass Fraction	Liquid Density
			kg/m ³
1	GASOLINE	1.0	
2			
3			
4			
5			

User Database

User Thermodynamic Property Database

Figure 40: Simulation Control: General Species Setup (Gasoline/Default).

Initialization (Gasoline)

Ratio A/F-Ratio

	Press.	Temp.	Fuel Vapour	Comb. Products	A/F-Ratio
	bar	degC	[-]	[-]	[-]
1	0.97	24.85	0	0	10000
2	0.95	24.85	0.074	0	10000
3	1.1	826.85	0	1	13.54
4	1.05	626.85	0	1	13.54
5					
6					
7					
8					

Figure 41: Simulation Control: General Species Setup - Initialization (Gasoline/Default).

System Boundary condition for intake (SB1) (Gasoline):

Boundary Conditions

Local Boundary Conditions

Preference

Pressure bar

Gas Temperature degC

Mass Fraction Input

Fuel Vapour [-]

Combustion Products [-]

Ratio Type

Ratio Value [-]

Global Boundary Conditions

Preference

Pressure	0.97	bar
Gas Temperature	24.85	degC
Fuel Vapour	0	
Combustion Products	0	
A/F-Ratio	10000	

To specify mass flow instead of pressure connect this element to an Engine Interface element with appropriate actuator channel.

Figure 42: System Boundary Condition for the intake (SB1) (Gasoline/Default).

Both flow coefficients are set with the value of 1.

System Boundary condition for the exhaust (SB2) (Gasoline):

Boundary Conditions

Local Boundary Conditions

Preference

Pressure bar

Gas Temperature degC

Mass Fraction Input

Fuel Vapour [-]

Combustion Products [-]

Ratio Type

Ratio Value [-]

Global Boundary Conditions

Preference

Pressure	0.97	bar
Gas Temperature	24.85	degC
Fuel Vapour	0	
Combustion Products	0	
A/F-Ratio	10000	

To specify mass flow instead of pressure connect this element to an Engine Interface element with appropriate actuator channel.

Figure 43: System Boundary Condition for the exhaust (SB2) (Gasoline/Default).

Both flow coefficients are set with the value of 1.

Injector (Gasoline)

General

Author
Comment
Result Name Date

Injection Method Continuous Intermittent
Reference Cylinder
Injection Angle (rel. to FTDC) deg SOI EOJ
Injector Rate/Duration Settings
Delivery Rate kg/s
Injection Duration s
Fuel Film Formation and Evaporation Specification
Fuel Film Thickness mm
Fuel Film Liquid Density kg/m³
Fraction of Fuel in Wallfilm [-]
Film=Wall Temperature taken from
Evaporation Multiplier [-]
Shape Multiplier [-]

Figure 44: Injector: General data (Gasoline/Default).

Mass Flow Specification

Ratio Control Direct Control

Ratio Control

Ratio [-]
Injector Model : Carburettor
 Injection Nozzle (Continuous Injection)
Air Flow taken from Measuring Point
The Injector Covers % of the Total Air Flow

Direct Control

Mass / Cycle kg/cycle
 Mass / Time kg/s

Figure 45: Injector: Mass Flow Specification (Gasoline/Default).

Both Flow Coefficients are set in 1.

Catalyst:

General

Author:

Comment:

Result Name: Date:

Chemical Reactions

Cycle Simulation: By enabling 'Chemical Reactions' the Catalyst model described in the Aftertreatment User Manual can be selected and the chemical processes can be modeled. By disabling this switch only the pressure drop of the Catalyst is going to be calculated.

Monolith Volume: l

Length of Monolith: mm

Inlet Collector Volume: l

Outlet Collector Volume: l

Couple to upstream element

Consider Air Gap between the Substrates

Figure 46: Catalyst: General (Gasoline/Default).

Type Specification

Catalyst Type Specification Square Cell Catalyst General Catalyst

Square Cell Catalyst

Cell Density (CPSI): 1/in²

Wall Thickness: mm

The input of the <Washcoat Thickness> is moved to the page <Washcoat>

General Catalyst

Open Frontal Area (OFA):

Hydraulic Unit

Diameter Area

Hydraulic Diameter: mm

Hydraulic Area: mm²

Geometrical Surface Area (GSA): 69.405394 1/m

Figure 47: Catalyst: Type Specification (Gasoline/Default).

Friction

Friction Specification Target Pressure Drop Coefficient

Target Pressure Drop

Inlet Massflow: kg/s

Inlet Temperature: degC

Inlet Pressure: bar

Target Pressure Drop: bar

Aftertreatment Analysis mode: Only the specification via <Friction Coefficient> is used!

Cycle Simulation mode: As Coefficient method only Darcy method supported. For laminar friction coefficient b only the default value (b=-1) is supported! Pressure Drop Multiplier is used only for Aftertreatment Analysis Simulation.

Figure 48: Catalyst: Friction (Gasoline/Default).

Results specification has the spatial position set at "Use 5 Points", and type of Results is set as "Standard". Every Flow Coefficient is set as 1.

Cylinder (Gasoline):

Initialization

Initial Conditions at EO

Pressure bar

Temperature degC

Initial Gas Composition

Ratio Type

Ratio Value [-]

Fuel Vapour [-]

Combustion Products [-]

SHP Condition Setting

Figure 49: Cylinder: Initialization (Gasoline/Default).

Combustion

Heat Release

Vibe Parameter Fitting

Fuelling

Fuel Mass / Cycle kg

A/F-Ratio [-]

Mixture Preparation

Internal External

The Mixture Preparation setting determines the treatment of in-cylinder evaporation and the local combustion excess air ratio development for 2-Zone combustion models (for details please refer to the Online Help).

Fuel Temperature degC

In Cylinder Evaporation

Evaporation Heat kJ/kg

Heat from Wall [-]

Figure 50: Cylinder: Combustion model (Gasoline/Default).

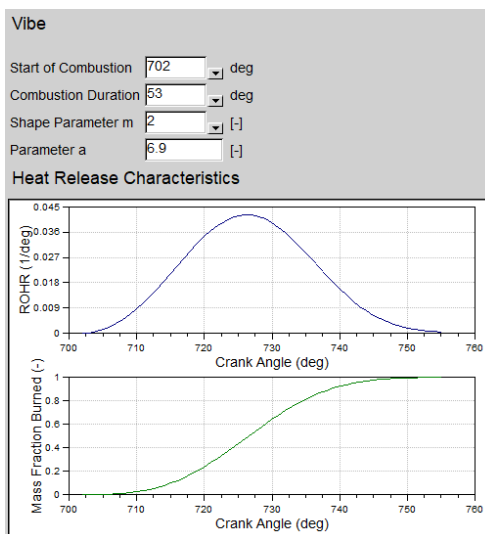


Figure 51: Cylinder: Vibe (Gasoline/Default).

For Hydrogen Model.

Set up simulation control (H₂):

General Species Setup

Species Set

	Species
1	HYDROGEN
2	O2
3	N2
4	CO2
5	H2O

Homogenous Reaction Set

	Key	Chemistry
1		
2		
3		
4		
5		

Insert Remove Load Store

Fuel Species Set

Mass Based Fractions Volume Based Fractions

	Fuel Species	Mass Fraction	Liquid Density kg/m ³
1	HYDROGEN	1.0	
2			
3			
4			
5			

Insert Remove Load Store

User Database

User Thermodynamic Property Database

Figure 52: Simulation Control: General Species Setup (H₂).

Initialization (H₂)

Ratio

	Press. bar	Temp. degC	Fuel Vapour [-]	Comb. Products [-]	A/F-Ratio [-]
1	0.97	24.85	0	0	10000
2	0.95	24.85	0.074	0	10000
3	1.1	826.85	0	1	34.2
4	1.05	626.85	0	1	34.2
5					
6					
7					
8					

Add Set Remove Set Load Store

Figure 53: Simulation Control: General Species Setup - Initialization (H₂).

System Boundary condition for intake (SB1) (H₂):

Boundary Conditions

Local Boundary Conditions

Preference: Set 1 [Update]

Pressure: 1 bar

Gas Temperature: 24.85 degC

Mass Fraction Input

Fuel Vapour: 0 [-]

Combustion Products: 0 [-]

Ratio Type: A/F - Ratio

Ratio Value: 10000 [-]

Global Boundary Conditions

Preference: Set 1

Pressure: 0.97 bar

Gas Temperature: 24.85 degC

Fuel Vapour: 0

Combustion Products: 0

A/F-Ratio: 10000

To specify mass flow instead of pressure connect this element to an Engine Interface element with appropriate actuator channel.

Figure 54: System Boundary Condition for the intake (SB1) (H2)

System Boundary condition for the exhaust (SB2) (H₂):

Boundary Conditions

Local Boundary Conditions

Preference: Set 1 [Update]

Pressure: 1 bar

Gas Temperature: 226.85 degC

Mass Fraction Input

Fuel Vapour: 0 [-]

Combustion Products: 1 [-]

Ratio Type: A/F - Ratio

Ratio Value: 34 [-]

Global Boundary Conditions

Preference: Set 1

Pressure: 0.97 bar

Gas Temperature: 24.85 degC

Fuel Vapour: 0

Combustion Products: 0

A/F-Ratio: 10000

To specify mass flow instead of pressure connect this element to an Engine Interface element with appropriate actuator channel.

Figure 55: System Boundary Condition for the exhaust (SB1) (H2).

Cylinder (H₂):

Initialization

Initial Conditions at EO

Pressure bar

Temperature degC

Initial Gas Composition

Ratio Type

Ratio Value [-]

Fuel Vapour [-]

Combustion Products [-]

SHP Condition Setting

Figure 56: Cylinder: Initialization (H₂).

Pollutants

Burned Zone Stratification Model

No. of zones

NOx Production Model

NOx Kinetic Multiplier [-]

NOx Postprocessing Multiplier [-]

CO Production Model

CO Kinetic Multiplier [-]

Soot Production Model

Soot Production Constant [-]

Soot Consumption Constant [-]

HC Production Model

Crevice height mm

Crevice gap mm

Oilfilm thickness mm

HC postoxidation multiplier [-]

HC postoxidation E degC

HC postoxidation f [-]

HC partial burn P [-]

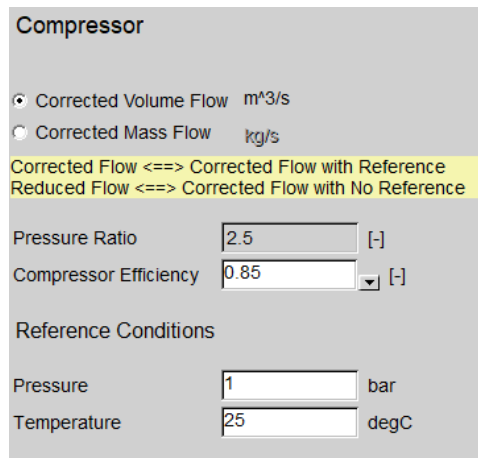
Figure 57: Cylinder: Pollutants (H₂).

List of Parameters:

- E_Speed: Engine Speed (rpm).
- I_Ratio: Injected Ratio.
- CR: Compression Ratio.
- Start_Comb: Start of the combustion (deg CA).
- Comb_Duration: Duration of the combustion (deg CA).
- Shape_Parameter_m: Vibe's Shape parameter m.
- Parameter_a: Vibe's parameter a.
- TC_PBoost: Turbocharger pressure ratio (aimed pressure boost).

For the Turbocharger, simplified model was chosen as the calculation type. Turbine layout calculation was the mode of calculation that was selected inside this model.

Then for Compressor:



Compressor

Corrected Volume Flow m^3/s
 Corrected Mass Flow kg/s

Corrected Flow <==> Corrected Flow with Reference
 Reduced Flow <==> Corrected Flow with No Reference

Pressure Ratio [-]

Compressor Efficiency [-]

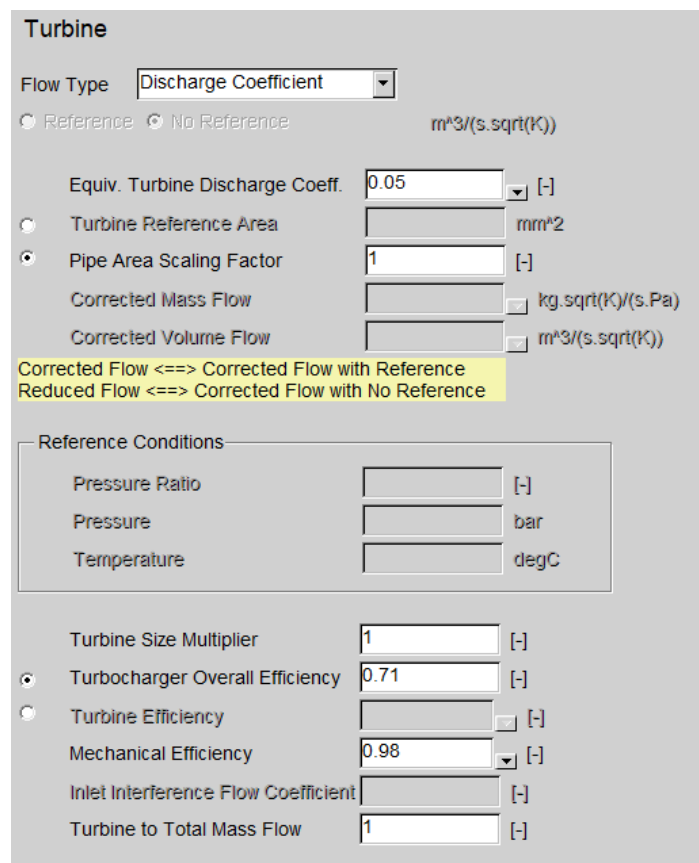
Reference Conditions

Pressure bar

Temperature degC

Figure 58: TC: Compressor (H_2)

For the Turbine:



Turbine

Flow Type

Reference No Reference $m^3/(s.\sqrt{K})$

Equiv. Turbine Discharge Coeff. [-]

Turbine Reference Area mm^2
 Pipe Area Scaling Factor [-]

Corrected Mass Flow $kg.\sqrt{K}/(s.Pa)$

Corrected Volume Flow $m^3/(s.\sqrt{K})$

Corrected Flow <==> Corrected Flow with Reference
 Reduced Flow <==> Corrected Flow with No Reference

Reference Conditions

Pressure Ratio [-]

Pressure bar

Temperature degC

Turbine Size Multiplier [-]

Turbocharger Overall Efficiency [-]
 Turbine Efficiency [-]

Mechanical Efficiency [-]

Inlet Interference Flow Coefficient [-]

Turbine to Total Mass Flow [-]

Figure 59: TC: Turbine (H_2)

For the Air Cooler:

General

Author: Marcos Mas
Comment:
Result Name:
Date: 29. Jun 2024

Geometrical Properties

Total Air Cooler Volume	10	l
Inlet Collector Volume	3	l
Outlet Collector Volume	3	l
Length of Cooling Core	600	mm

Hydraulic Setting of Cooling Core

Hydraulic Setting

Hydraulic Unit: Diameter Area

Hydraulic Diameter:
Hydraulic Area:
mm
mm²

Figure 60: Air Cooler: General (Geometry) (H₂).

Reference Operating Conditions

Friction Specification: Target Pressure Drop Coefficient

Heat Transfer Specification: Target Outlet Temperature Target Efficiency Heat Transfer Factor

Reference Operating Conditions

Mass Flow	0.333	kg/s
Inlet Air Temperature	141.85	degC
Inlet Pressure	1.5	bar

Friction

Target Pressure Drop	0.05	bar
Friction Coefficient		[-]
Lam. Friction Coeff.	64	[-]

Heat Transfer

Coolant Temperature	24.85	degC
Target Outlet Temperature	65	degC
Target Efficiency	0.65683761	[-]
Heat Transfer Factor	0	[-]

Figure 61: Air Cooler: Reference Operating Conditions (H₂)

Every Flow coefficient is set as 1.

ANNEX B: Vibe parameters fitted.

Case	E_Speed [rpm]	Lambda	a	b	CD [deg CA]	IT [deg CA]	m
1.1	2000	1.3	5.675	1071	15.89	717	2.085
1.2	2000	1.3	6.54	1071	16.49	717	2.085
1.3	2000	1.3	6.731	1071	16.62	717	2.085
2.1	2000	1.6	5.409	913.6	24.45	710.4	3.438
2.2	2000	1.6	4.698	913.6	23.68	710.4	3.438
2.3	2000	1.6	6.717	913.6	25.67	710.4	3.438
3.1	2000	2	4.886	807.1	27.13	713.3	1.895
3.2	2000	2	4.564	807.1	26.49	713.3	1.895
3.4	2000	2	2.763	807.1	22.28	713.3	1.895
3.3	2000	2	5.228	807.1	27.77	713.3	1.895
4.1	2000	2.4	5.932	730.7	39.52	712.8	1.158
4.2	2000	2.4	5.224	730.7	37.26	712.8	1.158
4.3	2000	2.4	2.056	730.7	24.19	712.8	1.158
4.4	2000	2.4	2.331	730.7	25.64	712.8	1.158
5.1	2000	2.8	3.91	668.1	44.29	708.2	1.356
5.2	2000	2.8	3.113	668.1	40.2	708.2	1.356
5.3	2000	2.8	3.846	668.1	43.98	708.2	1.356
5.4	2000	2.8	3.173	668.1	40.53	708.2	1.356
6.1.1	2000	3.4	2.833	508.2	55.98	712.2	0.7083
6.1.2	2000	3.4	2.249	508.2	48.9	712.2	0.7083
6.1.2	2000	3.4	4.478	508.2	73.19	712.2	0.7083
6.1.3	2000	3.4	4.618	508.2	74.52	712.2	0.7083
6.2.1	2000	3.4	3.235	430.2	47.62	709.9	1.189
6.2.2	2000	3.4	2.492	430.2	42.27	709.9	1.189
6.2.3	2000	3.4	2.789	430.2	44.5	709.9	1.189
6.2.4	2000	3.4	5.048	430.2	58.36	709.9	1.189
7.1	3000	2	6.133	1068	36.92	712.3	1.417
7.2	3000	2	3.294	1068	28.55	712.3	1.417
7.3	3000	2	5.379	1068	34.97	712.3	1.417
8.1	3000	2.2	5.243	1002	37.76	710.4	1.413
8.2	3000	2.2	5	1002	37.03	710.4	1.413
8.3	3000	2.2	6.869	1002	42.23	710.4	1.413
9.1	3000	2.4	2.745	953.4	30.32	711.3	1.039
9.2	3000	2.4	4.289	953.4	37.74	711.3	1.039
9.3	3000	2.4	5.274	953.4	41.77	711.3	1.039
10.1	3000	2.8	3.654	911.3	38.92	711.1	1.126
10.2	3000	2.8	4	911.3	40.62	711.1	1.126
10.3	3000	2.8	3.574	911.3	38.52	711.1	1.126
10.4	3000	2.8	4.94	911.3	44.86	711.1	1.126
11.1	3000	3.2	4.051	777.2	59.09	704.7	1.206
11.2	3000	3.2	4.188	777.2	59.99	704.7	1.206

Case	E_Speed [rpm]	Lambda	a	b	CD [deg CA]	IT [deg CA]	m
11.3	3000	3.2	5	777.2	65.01	704.7	1.206
11.4	3000	3.2	5.395	777.2	67.29	704.7	1.206
12.1.1	3000	3.5	2.425	567.4	56.12	698.3	1.677
12.1.2	3000	3.5	3.776	567.4	66.22	698.3	1.677
12.1.3	3000	3.5	5.697	567.4	77.21	698.3	1.677
12.2.1	3000	3.5	2.437	612	57.84	703	1.159
12.2.2	3000	3.5	3.266	612	66.25	703	1.159
12.2.3	3000	3.5	4.116	612	73.74	703	1.159

Table 10: The best results from the fitting script for the vibe function, from which correlations are extracted.

Cases 6.1. are fitted with all the points extract from the experimental curve.

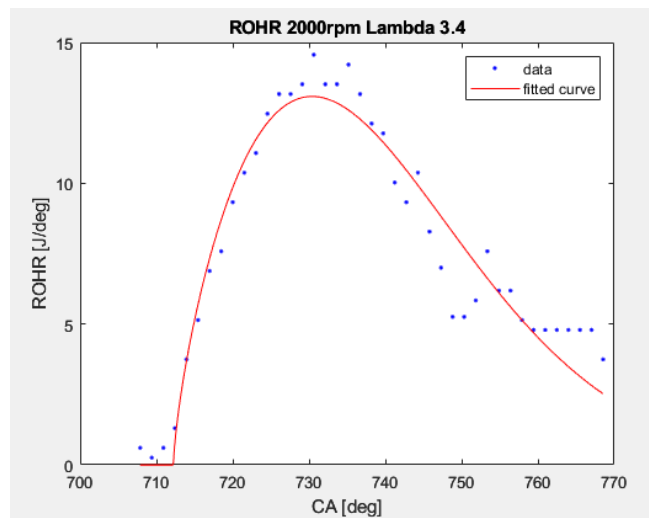


Figure 62: Comparison of the fitting curve and the data of 2000rpm and Lambda 3.4, considering every point of the data.

Case 6.2. are fitted without the data above 750.5 CA:

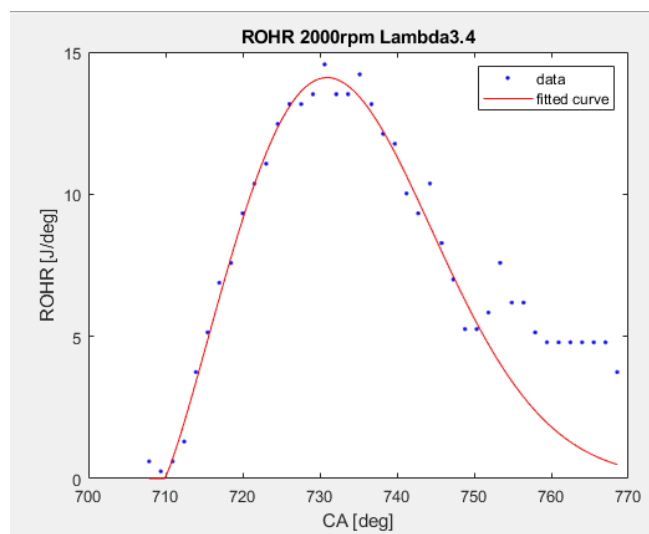


Figure 63: Comparison of the fitting curve and the data of 2000rpm and Lambda 3.4, without data above 756.6 CA.

Cases 12.1. are fitted without the data above 756.6 CA.

Cases 12.2 are fitted with all the date from the curve.

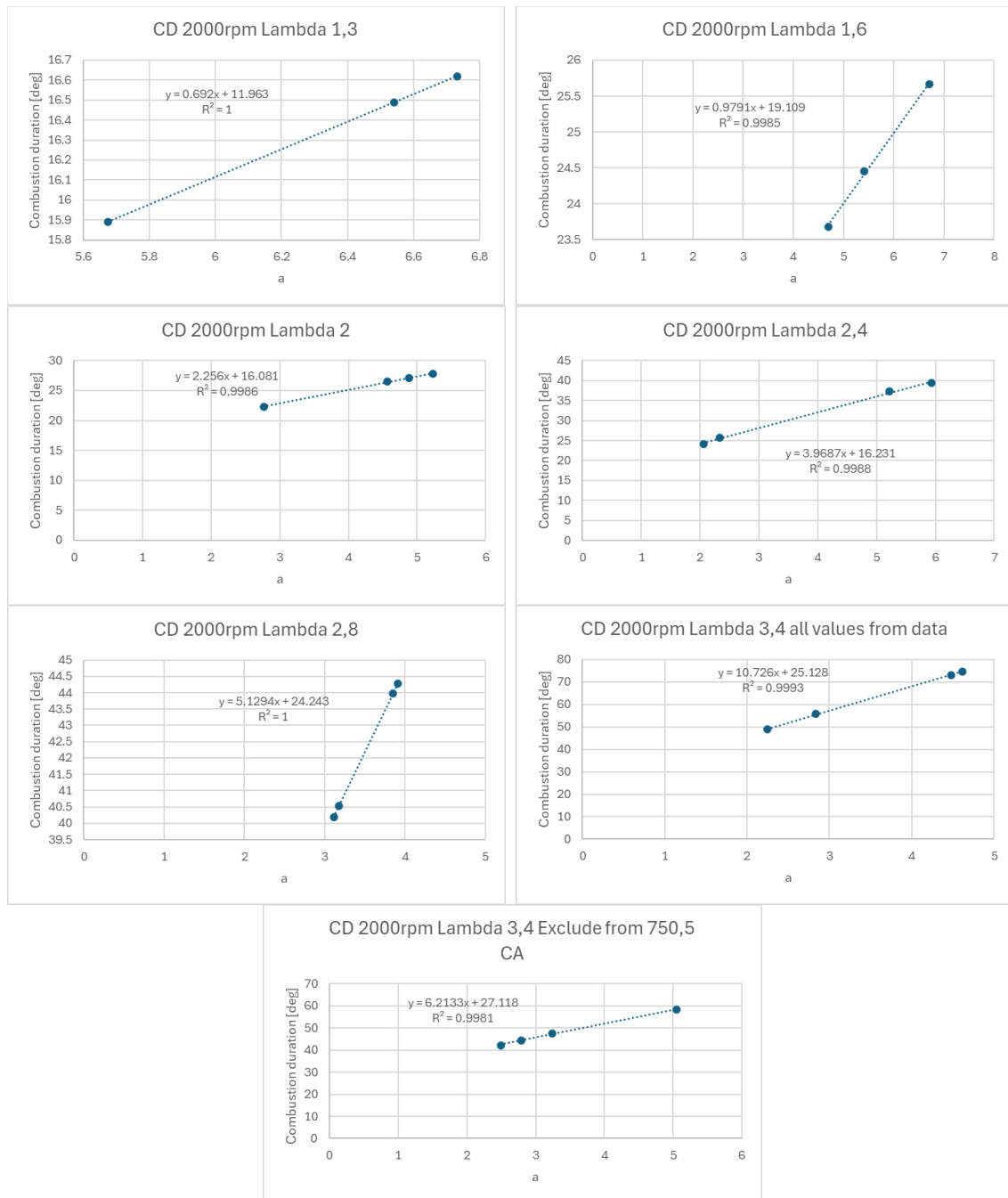


Figure 64: Graphical summary of the linear correlations between Parameter a and Combustion duration from fitting parameter at 2000 rpm and different lambdas.

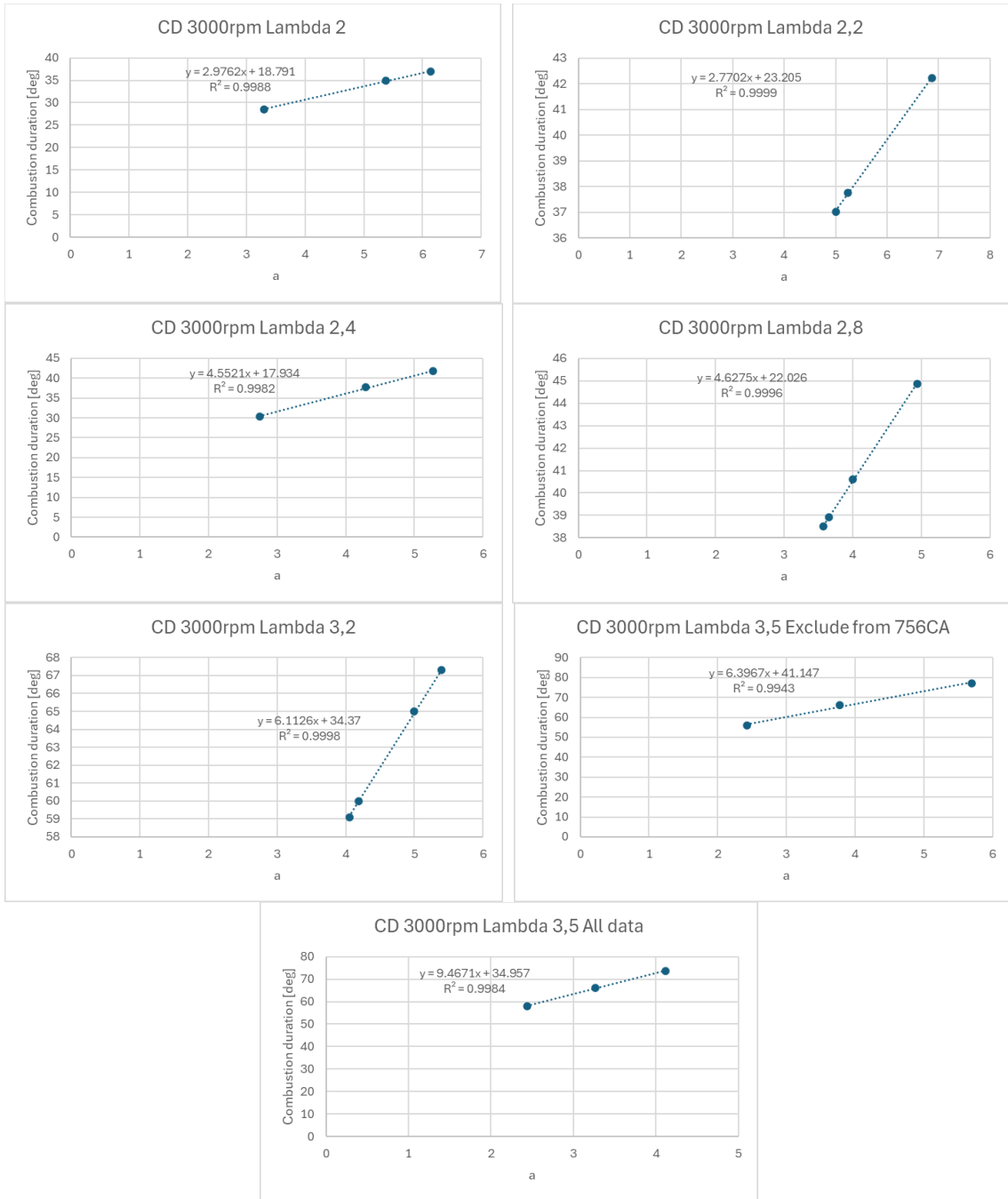


Figure 65: Graphical summary of the linear correlations between Parameter a and Combustion duration from fitting parameter at 3000 rpm and different lambdas.

ANNEX C: Simulation results gathered to evaluate the different approaches.

Table 11: Set 1: Efficiencies (Lean-burn approach).

Case	E_Speed	CR	Lambda	A/F_Ratio	Indicated Efficiency	Brake Efficiency	IMEP	BMEP
	[rpm]	(-)	(-)	(-)	(-)	(-)	[bar]	[bar]
Fit Vibe_2000rpm_L1_3	2000	11.5	1.3	44.59	0.4166	0.4005	10.652	9.643
Fit Vibe_2000rpm_L1_6	2000	11.5	1.6	54.88	0.4304	0.4027	8.991	7.982
Fit Vibe_2000rpm_L2	2000	11.5	2	68.6	0.4427	0.3994	7.454	6.444
Fit Vibe_2000rpm_L2_4	2000	11.5	2.4	82.32	0.4483	0.3913	6.335	5.323
Fit Vibe_2000rpm_L2_8	2000	11.5	2.8	96.04	0.4476	0.3790	5.461	4.448
Fit Vibe_2000rpm_L3_4_All	2000	11.5	3.4	116.62	0.4236	0.3386	4.305	3.291
Fit Vibe_3000rpm_L2	3000	11.5	2	68.6	0.4478	0.3937	7.705	6.397
Fit Vibe_3000rpm_L2_2	3000	11.5	2.2	75.46	0.4503	0.3892	7.076	5.768
Fit Vibe_3000rpm_L2_4	3000	11.5	2.4	82.32	0.4509	0.3822	6.525	5.217
Fit Vibe_3000rpm_L2_8	3000	11.5	2.8	96.04	0.4515	0.3697	5.648	4.341
Fit Vibe_3000rpm_L3_2	3000	11.5	3.2	109.76	0.4419	0.3470	4.884	3.577
Fit Vibe_3000rpm_L3_5_All	3000	11.5	3.5	120.05	0.4204	0.3160	4.289	2.983

Table 12: Set 1: Performance (Lean-burn approach).

Case	E_Speed	CR	Lambda	A/F_Ratio	Indicated Torque	Effective Torque	Indicated Power	Indicated Power2	Effective Power	Effective Power2
	[rpm]	(-)	(-)	(-)	[Nm]	[Nm]	[kW]	[PS]	[kW]	[PS]
Fit Vibe_2000rpm_L1_3	2000	11.5	1.3	44.59	41.69	38.27	8.73	11.87	8.02	10.90
Fit Vibe_2000rpm_L1_6	2000	11.5	1.6	54.88	35.09	31.68	7.35	9.99	6.64	9.02
Fit Vibe_2000rpm_L2	2000	11.5	2	68.6	28.99	25.57	6.07	8.25	5.36	7.28
Fit Vibe_2000rpm_L2_4	2000	11.5	2.4	82.32	24.54	21.13	5.14	6.99	4.42	6.02
Fit Vibe_2000rpm_L2_8	2000	11.5	2.8	96.04	21.07	17.65	4.41	6.00	3.70	5.03
Fit Vibe_2000rpm_L3_4_All	2000	11.5	3.4	116.62	16.47	13.06	4.69	4.69	2.74	3.72
Fit Vibe_3000rpm_L2	3000	11.5	2	68.6	29.44	25.39	9.25	12.57	7.98	10.85
Fit Vibe_3000rpm_L2_2	3000	11.5	2.2	75.46	26.94	22.89	8.46	11.51	7.19	9.78
Fit Vibe_3000rpm_L2_4	3000	11.5	2.4	82.32	24.75	20.71	7.78	10.57	6.50	8.84
Fit Vibe_3000rpm_L2_8	3000	11.5	2.8	96.04	21.28	17.23	6.68	9.09	5.41	7.36
Fit Vibe_3000rpm_L3_2	3000	11.5	3.2	109.76	18.25	14.20	5.73	7.79	4.46	6.06
Fit Vibe_3000rpm_L3_5_All	3000	11.5	3.5	120.05	15.89	11.84	4.99	6.79	3.72	5.06

Table 13: Set 1: NO_x Emissions (Lean-burn approach).

Case	E_Speed	CR	Lambda	A/F_Ratio	NO _x Classic		
	[rpm]	(-)	(-)	(-)	[g/kWh]	[g/h]	[ppm]
Fit Vibe_2000rpm_L1_3	2000	11.5	1.3	44.59	23.688	189.881	5635.65
Fit Vibe_2000rpm_L1_6	2000	11.5	1.6	54.88	8.541	56.669	1736.32
Fit Vibe_2000rpm_L2	2000	11.5	2	68.6	2.025	10.849	341.66
Fit Vibe_2000rpm_L2_4	2000	11.5	2.4	82.32	0.956	4.230	135.68
Fit Vibe_2000rpm_L2_8	2000	11.5	2.8	96.04	0.658	2.432	79.01
Fit Vibe_2000rpm_L3_4_All	2000	11.5	3.4	116.62	0.411	1.125	37.02
Fit Vibe_3000rpm_L2	3000	11.5	2	68.6	1.846	14.722	305.87
Fit Vibe_3000rpm_L2_2	3000	11.5	2.2	75.46	1.227	8.822	185.17
Fit Vibe_3000rpm_L2_4	3000	11.5	2.4	82.32	0.840	5.463	115.65
Fit Vibe_3000rpm_L2_8	3000	11.5	2.8	96.04	0.463	2.508	53.84
Fit Vibe_3000rpm_L3_2	3000	11.5	3.2	109.76	0.444	1.979	42.94
Fit Vibe_3000rpm_L3_5_All	3000	11.5	3.5	120.05	0.448	1.667	36.37

Table 14: General Gasoline engine Results.

Case	E_Speed	CR	Lambda	A/F_Ratio	Indicated Efficiency	Brake Efficiency	IMEP	BMEP	Effective Torque	Effective Power	NO _x Classic		
	[rpm]										(-)	(-)	(-)
G1	1500	9	1.05	15.33	0.3654	0.3332	9.439	8.609	34.17	5.37	13.768	73.897	630.49
G2	2000	9	1.05	15.33	0.3717	0.3354	9.826	8.866	35.19	7.37	13.763	101.437	778.55
G3	2500	9	1.05	15.33	0.3719	0.3303	9.739	8.649	34.33	8.99	13.386	120.298	824.24
G4	3000	9	1.05	15.33	0.3703	0.3225	9.462	8.242	32.71	10.28	12.683	130.343	847.41
G5	3500	9	1.05	15.33	0.3663	0.3126	9.205	7.855	31.18	11.43	12.016	137.303	861.11

Table 15: Set 2: Efficiencies (Compression Ratio Reduction)

Case	E_Speed	CR	Lambda	A/F_Ratio	Indicated Efficiency	Brake Efficiency	IMEP	BMEP
	[rpm]	(-)	(-)	(-)	(-)	(-)	[bar]	[bar]
Fit Vibe_2000rpm_L2_CR9	2000	9	2	68.6	0.4230	0.3804	7.214	6.205
Fit Vibe_2000rpm_L2_CR10	2000	10	2	68.6	0.4322	0.3893	7.329	6.319
Fit Vibe_2000rpm_L2	2000	11.5	2	68.6	0.4427	0.3994	7.454	6.444
Fit Vibe_2000rpm_L2_CR11	2000	11	2	68.6	0.4396	0.3964	7.418	6.407
Fit Vibe_2000rpm_L2_CR12	2000	12	2	68.6	0.4455	0.4020	7.486	6.476
Fit Vibe_2000rpm_L2_CR13	2000	13	2	68.6	0.4502	0.4064	7.539	6.528

Table 16: Set 2: Performance (CRR)

Case	E_Speed	CR	Lambda	A/F_Ratio	Indicated Torque	Effective Torque	Indicated Power	Indicated Power2	Effective Power	Effective Power2
	[rpm]	(-)	(-)	(-)	[Nm]	[Nm]	[kW]	[PS]	[kW]	[PS]
Fit Vibe_2000rpm_L2_CR9	2000	9	2	68.6	28.04	24.63	5.87	7.98	5.16	7.01
Fit Vibe_2000rpm_L2_CR10	2000	10	2	68.6	28.49	25.08	5.97	8.11	5.25	7.14
Fit Vibe_2000rpm_L2	2000	11.5	2	68.6	28.99	25.57	6.07	8.25	5.36	7.28
Fit Vibe_2000rpm_L2_CR11	2000	11	2	68.6	28.84	25.43	6.04	8.21	5.33	7.24
Fit Vibe_2000rpm_L2_CR12	2000	12	2	68.6	29.11	25.70	6.10	8.29	5.38	7.32
Fit Vibe_2000rpm_L2_CR13	2000	13	2	68.6	29.32	25.91	6.14	8.35	5.43	7.38

Table 17: Set 2: NO_x Emissions (CRR)

Case	E_Speed	CR	Lambda	A/F_Ratio	NO _x Classic		
	[rpm]	(-)	(-)	(-)	[g/kWh]	[g/h]	[ppm]
Fit Vibe_2000rpm_L2_CR9	2000	9	2	68.6	1.352	6.972	217.88
Fit Vibe_2000rpm_L2_CR10	2000	10	2	68.6	1.612	8.466	265.50
Fit Vibe_2000rpm_L2	2000	11.5	2	68.6	2.025	10.849	341.66
Fit Vibe_2000rpm_L2_CR11	2000	11	2	68.6	1.885	10.039	315.73
Fit Vibe_2000rpm_L2_CR12	2000	12	2	68.6	2.169	11.673	368.06
Fit Vibe_2000rpm_L2_CR13	2000	13	2	68.6	2.461	13.355	421.98

Table 18: Set 3: Efficiencies (TCI)

Case	E_Speed	CR	Lambda	A/F_Ratio	Pressure Boost	Indicated Efficiency	Brake Efficiency	IMEP	BMEP
	[rpm]	(-)	(-)	(-)	[bar]	(-)	(-)	[bar]	[bar]
TCI_Fit Vibe_2000rpm_L2_PB1-5	2000	11.5	2	68.6	1.4805	0.4683	0.4453	11.994	11.407
TCI_Fit Vibe_2000rpm_L2_PB2	2000	11.5	2	68.6	1.9651	0.4761	0.4615	15.879	15.556
TCI_Fit Vibe_2000rpm_L2_PB2-5	2000	11.5	2	68.6	2.4429	0.4783	0.4689	19.659	19.486
TCI_Fit Vibe_3000rpm_L2_PB1-5	3000	11.5	2	68.6	1.4538	0.4641	0.4393	14.376	13.219
TCI_Fit Vibe_3000rpm_L2_PB2	3000	11.5	2	68.6	1.9105	0.4674	0.4508	18.892	17.728
TCI_Fit Vibe_3000rpm_L2_PB2-5	3000	11.5	2	68.6	2.3450	0.4679	0.4559	23.194	21.920

Table 19: Set 3: Performance (TCI)

Case	E_Speed	CR	Lambda	A/F_Ratio	Pressure Boost	Indicated Torque	Effective Torque	Indicated Power	Indicated Power2	Effective Power	Effective Power2
	[rpm]	(-)	(-)	(-)	[bar]	[Nm]	[Nm]	[kW]	[PS]	[kW]	[PS]
TCI_Fit Vibe_2000rpm_L2_PB1-5	2000	11.5	2	68.6	1.4805	48.69	45.27	10.20	13.86	9.48	12.89
TCI_Fit Vibe_2000rpm_L2_PB2	2000	11.5	2	68.6	1.9651	65.16	61.74	13.65	18.55	12.93	17.58
TCI_Fit Vibe_2000rpm_L2_PB2-5	2000	11.5	2	68.6	2.4429	80.75	77.34	16.91	23.00	16.20	22.02
TCI_Fit Vibe_3000rpm_L2_PB1-5	3000	11.5	2	68.6	1.4538	56.51	52.46	17.75	24.14	16.48	22.41
TCI_Fit Vibe_3000rpm_L2_PB2	3000	11.5	2	68.6	1.9105	74.41	70.36	23.38	31.78	22.10	30.05
TCI_Fit Vibe_3000rpm_L2_PB2-5	3000	11.5	2	68.6	2.3450	91.05	87.00	28.60	38.89	27.33	37.16

Table 20: Set 3: NOx Emissions (TCI)

Case	E_Speed	CR	Lambda	A/F_Ratio	Pressure Boost	NO _x Classic		
	[rpm]	(-)	(-)	(-)	[bar]	[g/kWh]	[g/h]	[ppm]
TCI_Fit Vibe_2000rpm_L2_PB1-5	2000	11.5	2	68.6	1.4805	2.897	27.466	531.66
TCI_Fit Vibe_2000rpm_L2_PB2	2000	11.5	2	68.6	1.9651	3.467	44.829	656.58
TCI_Fit Vibe_2000rpm_L2_PB2-5	2000	11.5	2	68.6	2.4429	4.029	65.267	773.50
TCI_Fit Vibe_3000rpm_L2_PB1-5	3000	11.5	2	68.6	1.4538	3.166	52.184	580.08
TCI_Fit Vibe_3000rpm_L2_PB2	3000	11.5	2	68.6	1.9105	3.744	82.749	701.14
TCI_Fit Vibe_3000rpm_L2_PB2-5	3000	11.5	2	68.6	2.3450	4.207	114.979	796.35

Table 21: Set 4: Efficiencies (TCI + CRR)

Case	E_Speed	CR	Lambda	A/F_Ratio	Pressure Boost	Indicated Efficiency	Brake Efficiency	IMEP	BMEP
	[rpm]	(-)	(-)	(-)	[bar]	(-)	(-)	[bar]	[bar]
TCI_Fit Vibe_2000rpm_L2_PB1-5_CR9	2000	9	2	68.6	1.4801	0.4473	0.4251	11.683	11.104
TCI_Fit Vibe_2000rpm_L2_PB2_CR9	2000	9	2	68.6	1.9643	0.4557	0.4418	15.459	15.196
TCI_Fit Vibe_2000rpm_L2_PB2-5_CR9	2000	9	2	68.6	2.4414	0.4587	0.4497	19.128	19.076
TCI_Fit Vibe_3000rpm_L2_PB1-5_CR9	3000	9	2	68.6	1.4531	0.4405	0.4163	13.899	12.750
TCI_Fit Vibe_3000rpm_L2_PB2_CR9	3000	9	2	68.6	1.909	0.4446	0.4283	18.326	17.213
TCI_Fit Vibe_3000rpm_L2_PB2-5_CR9	3000	9	2	68.6	2.3425	0.4455	0.4337	22.538	21.359

Table 22: Set 4: Performance (TCI + CRR).

Case	E_Speed	CR	Lambda	A/F_Ratio	Pressure Boost	Indicated Torque	Effective Torque	Indicated Power	Indicated Power2	Effective Power	Effective Power2
	[rpm]	(-)	(-)	(-)	[bar]	[Nm]	[Nm]	[kW]	[PS]	[kW]	[PS]
TCI_Fit Vibe_2000rpm_L2_PB1-5_CR9	2000	9	2	68.6	1.4801	47.48	44.07	9.94	13.52	9.23	12.55
TCI_Fit Vibe_2000rpm_L2_PB2_CR9	2000	9	2	68.6	1.9643	63.73	60.31	13.35	18.15	12.63	17.17
TCI_Fit Vibe_2000rpm_L2_PB2-5_CR9	2000	9	2	68.6	2.4414	79.13	75.71	16.57	22.53	15.86	21.56
TCI_Fit Vibe_3000rpm_L2_PB1-5_CR9	3000	9	2	68.6	1.4531	54.65	50.60	17.17	23.34	15.90	21.61
TCI_Fit Vibe_3000rpm_L2_PB2_CR9	3000	9	2	68.6	1.909	72.37	68.32	22.74	30.91	21.46	29.18
TCI_Fit Vibe_3000rpm_L2_PB2-5_CR9	3000	9	2	68.6	2.3425	88.82	84.77	27.90	37.94	26.63	36.21

Table 23: Set 4: NO_x Emissions (TCI + CRR).

Case	E_Speed	CR	Lambda	A/F_Ratio	Pressure Boost	NO _x Classic		
	[rpm]	(-)	(-)	(-)	[bar]	[g/kWh]	[g/h]	[ppm]
TCI_Fit Vibe_2000rpm_L2_PB1-5_CR9	2000	9	2	68.6	1.4801	2.028	18.723	356.69
TCI_Fit Vibe_2000rpm_L2_PB2_CR9	2000	9	2	68.6	1.9643	2.456	31.020	446.76
TCI_Fit Vibe_2000rpm_L2_PB2-5_CR9	2000	9	2	68.6	2.4414	2.882	45.703	532.46
TCI_Fit Vibe_3000rpm_L2_PB1-5_CR9	3000	9	2	68.6	1.4531	2.173	34.540	378.51
TCI_Fit Vibe_3000rpm_L2_PB2_CR9	3000	9	2	68.6	1.909	2.598	55.756	464.00
TCI_Fit Vibe_3000rpm_L2_PB2-5_CR9	3000	9	2	68.6	2.3425	2.949	78.535	532.94

Table 24: Set 5: Efficiencies (TCI + Lean-burn).

Case	E_Speed	CR	Lambda	A/F_Ratio	Pressure Boost	Indicated Efficiency	Brake Efficiency	IMEP	BMEP
	[rpm]	(-)	(-)	(-)	[bar]	(-)	(-)	[bar]	[bar]
TCI_Vibe_2000rpm_L2_8_PB1-5	2000	11.5	2.8	96.04	1.4805	0.4769	0.4354	8.754	8.083
TCI_Fit Vibe_2000rpm_L2_8_PB2	2000	11.5	2.8	96.04	1.9653	0.4809	0.4507	11.588	11.017
TCI_Fit Vibe_2000rpm_L2_8_PB2-5	2000	11.5	2.8	96.04	2.4441	0.4828	0.4592	14.549	14.017
TCI_Fit Vibe_3000rpm_L2_8_PB1-5	3000	11.5	2.8	96.04	1.4539	0.4668	0.4251	10.542	9.263
TCI_Fit Vibe_3000rpm_L2_8_PB2	3000	11.5	2.8	96.04	1.9111	0.4680	0.4374	13.875	12.474
TCI_Fit Vibe_3000rpm_L2_8_PB2-5	3000	11.5	2.8	96.04	2.3521	0.4681	0.4446	17.291	15.692

Table 25: Set 5: Performance (TCI + Lean-burn).

Case	E_Speed	CR	Lambda	A/F_Ratio	Pressure Boost	Indicated Torque	Effective Torque	Indicated Power	Indicated Power2	Effective Power	Effective Power2
	[rpm]	(-)	(-)	(-)	[bar]	[Nm]	[Nm]	[kW]	[PS]	[kW]	[PS]
TCI_Vibe_2000rpm_L2_8_PB1-5	2000	11.5	2.8	96.04	1.4805	35.49	32.08	7.43	10.11	6.72	9.13
TCI_Fit Vibe_2000rpm_L2_8_PB2	2000	11.5	2.8	96.04	1.9653	47.14	43.73	9.87	13.42	9.16	12.45
TCI_Fit Vibe_2000rpm_L2_8_PB2-5	2000	11.5	2.8	96.04	2.4441	59.05	55.63	12.37	16.81	11.65	15.84
TCI_Fit Vibe_3000rpm_L2_8_PB1-5	3000	11.5	2.8	96.04	1.4539	40.81	36.76	12.82	17.43	11.55	15.70
TCI_Fit Vibe_3000rpm_L2_8_PB2	3000	11.5	2.8	96.04	1.9111	53.56	49.51	16.83	22.88	15.55	21.15
TCI_Fit Vibe_3000rpm_L2_8_PB2-5	3000	11.5	2.8	96.04	2.3521	66.33	62.28	20.84	28.33	19.57	26.60

Table 26: Set 5: NO_x Emissions (TCI + Lean-burn)

Case	E_Speed	CR	Lambda	A/F_Ratio	Pressure Boost	NO _x Classic		
	[rpm]	(-)	(-)	(-)	[bar]	[g/kWh]	[g/h]	[ppm]
TCI_Vibe_2000rpm_L2_8_PB1-5	2000	11.5	2.8	96.04	1.4805	0.885	5.948	118.69
TCI_Fit Vibe_2000rpm_L2_8_PB2	2000	11.5	2.8	96.04	1.9653	1.051	9.623	145.16
TCI_Fit Vibe_2000rpm_L2_8_PB2-5	2000	11.5	2.8	96.04	2.4441	1.174	13.680	165.35
TCI_Fit Vibe_3000rpm_L2_8_PB1-5	3000	11.5	2.8	96.04	1.4539	0.792	9.142	104.40
TCI_Fit Vibe_3000rpm_L2_8_PB2	3000	11.5	2.8	96.04	1.9111	0.917	14.265	124.22
TCI_Fit Vibe_3000rpm_L2_8_PB2-5	3000	11.5	2.8	96.04	2.3521	0.981	19.194	135.05

Table 27: Set 6: Efficiencies (TCI+CRR+Lean burn $\lambda = 2.8$).

Case	E_Speed	CR	Lambda	A/F_Ratio	Pressure Boost	Indicated Efficiency	Brake Efficiency	IMEP	BMEP
	[rpm]	(-)	(-)	(-)	[bar]	(-)	(-)	[bar]	[bar]
TCI_Vibe_2000rpm_L2_8_PB1-5_CR9	2000	9	2.8	96.04	1.4802	0.4570	0.4166	8.538	7.901
TCI_Fit Vibe_2000rpm_L2_8_PB2_CR9	2000	9	2.8	96.04	1.9646	0.4622	0.4327	11.306	10.822
TCI_Fit Vibe_2000rpm_L2_8_PB2-5_CR9	2000	9	2.8	96.04	2.4428	0.4643	0.4413	14.223	13.818
TCI_Fit Vibe_3000rpm_L2_8_PB1-5_CR9	3000	9	2.8	96.04	1.4532	0.4444	0.4035	10.210	8.956
TCI_Fit Vibe_3000rpm_L2_8_PB2_CR9	3000	9	2.8	96.04	1.9093	0.4455	0.4155	13.430	12.075
TCI_Fit Vibe_3000rpm_L2_8_PB2-5_CR9	3000	9	2.8	96.04	2.3501	0.4453	0.4224	16.735	15.185

Table 28: Set 6: Performance (TCI+CRR+Lean burn $\lambda = 2.8$).

Case	E_Speed	CR	Lambda	A/F_Ratio	Pressure Boost	Indicated Torque	Effective Torque	Indicated Power	Indicated Power2	Effective Power	Effective Power2
	[rpm]	(-)	(-)	(-)	[bar]	[Nm]	[Nm]	[kW]	[PS]	[kW]	[PS]
TCI_Vibe_2000rpm_L2_8_PB1-5_CR9	2000	9	2.8	96.04	1.4802	34.77	31.36	7.28	9.90	6.57	8.93
TCI_Fit Vibe_2000rpm_L2_8_PB2_CR9	2000	9	2.8	96.04	1.9646	46.36	42.95	9.71	13.20	9.00	12.23
TCI_Fit Vibe_2000rpm_L2_8_PB2-5_CR9	2000	9	2.8	96.04	2.4428	58.26	54.84	12.20	16.59	11.49	15.62
TCI_Fit Vibe_3000rpm_L2_8_PB1-5_CR9	3000	9	2.8	96.04	1.4532	39.59	35.55	12.44	16.91	11.17	15.18
TCI_Fit Vibe_3000rpm_L2_8_PB2_CR9	3000	9	2.8	96.04	1.9093	51.97	47.92	16.33	22.20	15.06	20.47
TCI_Fit Vibe_3000rpm_L2_8_PB2-5_CR9	3000	9	2.8	96.04	2.3501	64.32	60.27	20.21	27.47	18.93	25.74

Table 29 Set 6: NO_x Emissions (TCI+CRR+Lean burn $\lambda = 2.8$).

Case	E_Speed	CR	Lambda	A/F_Ratio	Pressure Boost	NO _x Classic		
	[rpm]	(-)	(-)	(-)	[bar]	[g/kWh]	[g/h]	[ppm]
TCI_Vibe_2000rpm_L2_8_PB1-5_CR9	2000	9	2.8	96.04	1.4802	0.536	3.518	69.12
TCI_Fit Vibe_2000rpm_L2_8_PB2_CR9	2000	9	2.8	96.04	1.9646	0.646	5.807	86.08
TCI_Fit Vibe_2000rpm_L2_8_PB2-5_CR9	2000	9	2.8	96.04	2.4428	0.728	8.363	99.02
TCI_Fit Vibe_3000rpm_L2_8_PB1-5_CR9	3000	9	2.8	96.04	1.4532	0.469	5.237	59.01
TCI_Fit Vibe_3000rpm_L2_8_PB2_CR9	3000	9	2.8	96.04	1.9093	0.547	8.241	70.72
TCI_Fit Vibe_3000rpm_L2_8_PB2-5_CR9	3000	9	2.8	96.04	2.3501	0.578	10.949	75.80

Table 30: Set 6: Efficiencies (TCI+CRR+Lean burn $\lambda = 3.4$).

Case	E_Speed	CR	Lambda	A/F_Ratio	Pressure Boost	Indicated Efficiency	Brake Efficiency	IMEP	BMEP
	[rpm]	(-)	(-)	(-)	[bar]	(-)	(-)	[bar]	[bar]
TCI_Vibe_2000rpm_L3_5_PB1-5_CR9	2000	9	3.4	116.62	1.4802	0.4370	0.3857	6.723	6.047
TCI_Fit Vibe_2000rpm_L3_5_PB2_CR9	2000	9	3.4	116.62	1.9647	0.4401	0.4021	8.888	8.305
TCI_Fit Vibe_2000rpm_L3_5_PB2-5_CR9	2000	9	3.4	116.62	2.4431	0.4411	0.4110	11.167	10.618
TCI_Fit Vibe_3000rpm_L3_5_PB1-5_CR9	3000	9	3.5	120.05	1.4533	0.4156	0.3619	7.771	6.464
TCI_Fit Vibe_3000rpm_L2_8_PB2_CR9	3000	9	3.5	120.05	1.9096	0.4154	0.3751	10.211	8.766
TCI_Fit Vibe_3000rpm_L3_5_PB2-5_CR9	3000	9	3.5	120.05	2.3504	0.4143	0.3827	12.724	11.068

Table 31: Set 6: Performance (TCI+CRR+Lean burn $\lambda = 3.4$)

Case	E_Speed	CR	Lambda	A/F_Ratio	Indicated Torque	Effective Torque	Indicated Power	Indicated Power2	Effective Power	Effective Power2
	[rpm]	(-)	(-)	(-)	[Nm]	[Nm]	[kW]	[PS]	[kW]	[PS]
TCI_Vibe_2000rpm_L3_5_PB1-5_CR9	2000	9	3.4	116.62	27.41	24.00	5.74	7.81	5.03	6.83
TCI_Fit Vibe_2000rpm_L3_5_PB2_CR9	2000	9	3.4	116.62	36.38	32.96	7.62	10.36	6.90	9.39
TCI_Fit Vibe_2000rpm_L3_5_PB2-5_CR9	2000	9	3.4	116.62	45.56	42.14	9.54	12.97	8.83	12.00
TCI_Fit Vibe_3000rpm_L3_5_PB1-5_CR9	3000	9	3.5	120.05	29.70	25.66	9.33	12.69	8.06	10.96
TCI_Fit Vibe_3000rpm_L2_8_PB2_CR9	3000	9	3.5	120.05	38.84	34.79	12.20	16.59	10.93	14.86
TCI_Fit Vibe_3000rpm_L3_5_PB2-5_CR9	3000	9	3.5	120.05	47.98	43.93	15.07	20.49	13.80	18.76

Table 32: Set 6: NO_x Emissions (TCI+CRR+Lean burn $\lambda = 3.4$).

Case	E_Speed	CR	Lambda	A/F_Ratio	Pressure Boost	NO _x Classic		
	[rpm]	(-)	(-)	(-)	[bar]	[g/kWh]	[g/h]	[ppm]
TCI_Vibe_2000rpm_L3_5_PB1-5_CR9	2000	9	3.4	116.62	1.4802	0.312	1.568	31.25
TCI_Fit Vibe_2000rpm_L3_5_PB2_CR9	2000	9	3.4	116.62	1.9647	0.372	2.569	38.66
TCI_Fit Vibe_2000rpm_L3_5_PB2-5_CR9	2000	9	3.4	116.62	2.4431	0.415	3.664	44.11
TCI_Fit Vibe_3000rpm_L3_5_PB1-5_CR9	3000	9	3.5	120.05	1.4533	0.413	3.328	38.08
TCI_Fit Vibe_3000rpm_L2_8_PB2_CR9	3000	9	3.5	120.05	1.9096	0.476	5.201	45.40
TCI_Fit Vibe_3000rpm_L3_5_PB2-5_CR9	3000	9	3.5	120.05	2.3504	0.504	6.959	49.08

